PERGAMON

Quaternary Science Reviews 20 (2001) 659–678

QSR

A multiproxy reconstruction of the evolution of deep and surface waters in the subarctic Nordic seas over the last 30,000 yr

Henning A. Bauch[a,*], Helmut Erlenkeuser[b], Robert F. Spielhagen[a], Ulrich Struck[c], Jens Matthiessen[d], Jörn Thiede[d], Jan Heinemeier[e]

[a]*GEOMAR, Research Center for Marine Geosciences, University of Kiel, Wischhofstrasse 1-3, 24148 Kiel, Germany*
[b]*Leibniz Laboratory, University of Kiel, 24098 Kiel, Germany*
[c]*Institute of Paleontology, University of München, Richard-Wagner-Strasse 10, 80333 München, Germany*
[d]*Alfred Wegener Institute for Polar and Marine Research, Columbusstrasse, 27568 Bremerhaven, Germany*
[e]*Institute for Physics and Astronomy, University of Aarhus, 8000 Aarhus, Denmark*

Abstract

On the basis of various lithological, mircopaleontological and isotopic proxy records covering the last 30,000 calendar years (cal kyr) the paleoenvironmental evolution of the deep and surface water circulation in the subarctic Nordic seas was reconstructed for a climate interval characterized by intensive ice-sheet growth and subsequent decay on the surrounding land masses. The data reveal considerable temporal changes in the type of thermohaline circulation. Open-water convection prevailed in the early record, providing moisture for the Fennoscandian-Barents ice sheets to grow until they reached the shelf break at $\sim$26 cal. kyr and started to deliver high amounts of ice-rafted debris (IRD) into the ocean via melting icebergs. Low epibenthic $\delta^{18}O$ values and small-sized subpolar foraminifera observed after 26 cal. kyr may implicate that advection of Atlantic water into the Nordic seas occurred at the subsurface until 15 cal. kyr. Although modern-like surface and deep-water conditions first developed at $\sim$13.5 cal. kyr, thermohaline circulation remained unstable, switching between a subsurface and surface advection of Atlantic water until 10 cal. kyr when IRD deposition and major input of meltwater ceased. During this time, two depletions in epibenthic $\delta^{13}C$ are recognized just before and after the Younger Dryas indicating a notable reduction in convectional processes. Despite an intermittent cooling at $\sim$8 cal. kyr, warmest surface conditions existed in the central Nordic seas between 10 and 6 cal. kyr. However, already after 7 cal. kyr the present day situation gradually evolved, verified by a strong water mass exchange with the Arctic Ocean and an intensifying deep convection as well as surface temperature decrease in the central Nordic seas. This process led to the development of the modern distribution of water masses and associated oceanographic fronts after 5 cal. kyr and, eventually, to today's steep east–west surface temperature gradient. The time discrepancy between intensive vertical convection after 5 cal. kyr but warmest surface temperatures already between 10 and 6 cal. kyr strongly implicates that widespread postglacial surface warming in the Nordic seas was not directly linked to the rates in deep-water formation.

1. Introduction

Paleoceanographic studies have demonstrated that the oceanic circulation in the North Atlantic region was quite variable between the Lateglacial and Holocene periods (e.g., Broecker et al., 1988; Lehman and Keigwin, 1992; Veum et al., 1992). Salinity changes in regions of thermohaline circulation and deep-water formation have been proposed for being partly responsible for these rapid climatic shifts (Broecker et al., 1990; Rahmstorf, 1995). Sediment cores from the North Atlantic document that Last Glacial ice-sheets fluctuated in size on time-scales not recognized previously (Bond and Lotti, 1995), and that such fluctuations were probably also causing some of the salinity changes at these mid- to high-northern latitudes due to enhanced iceberg thawing (e.g., Duplessy et al., 1991; Bond et al., 1993; Maslin et al., 1995).

The Norwegian–Greenland–Iceland seas (Nordic seas) is a region well suited to study glacial to interglacial climatic changes. This is because intense deep-water formation occurs here as a result of the poleward flow of warm and saline Atlantic surface water and consequent cooling of these waters upon heat release. This process is recognized as an integral part of the modern, interglacial climate system. It is believed that the present day situation, with barely any ice left in Scandinavia, is the result

* Corresponding author. Tel.: 49-431-600-2853; fax: 49-431-600-2941.
E-mail address: hbauch@geomar.de (H.A. Bauch).

0277-3791/01/$ - see front matter
PII: S0277-3791(00)00098-6

of the global climate change after the Last Glacial Maximum (LGM) triggered by an increasing solar radiance and a subsequent northward expansion of warm Atlantic surface waters into subarctic latitudes (Ruddiman and McIntyre, 1981; Imbrie et al., 1993). During the LGM, the landmasses surrounding the Nordic seas were largely covered by ice sheets. At this time and during the ensuing deglacial phase planktic foraminiferal isotopes and sedimentologic proxies show that the marginal regions of the Nordic seas have repeatedly received high but also variable amounts of sediments from icebergs/ice-sheet magins (e.g., Elverhøi et al., 1995; Laberg and Vorren, 1995), and that strongly varying surface salinity conditions due to meltwater input probably had a pronounced effect on the surface circulation and intensity of deep-water renewal (e.g., Veum et al., 1992; Sarnthein et al., 1995). The water-mass variability at the surface, particularly during the last deglaciation, apparently paralleled rapid atmospheric temperature changes on the nearby ice-covered landmasses (e.g., Lehman and Keigwin, 1992; Taylor et al., 1993).

1.1. Rationale

Supported by planktic stable isotope studies, micropaleontological records have been used in the Nordic seas to elucidate past water mass changes in the Nordic seas (Kellogg, 1980; Jansen and Bjørklund, 1985; Baumann and Matthiessen, 1992; Koç-Karpuz and Jansen, 1992; Sarnthein et al., 1995; Hald et al., 1996). Despite considerable progress in the understanding of the glacial-to-interglacial climate system has been made on the basis of these studies, they could only partially unveal the specific conditions of the LGM. Previous interpretations saw the Nordic seas as an ice-covered region during the LGM. But more recent investigations suggest the presence of Atlantic surface water as well as open-water conditions during the main glacial phase, oxygen isotope stage (OIS) 2 (Bauch, 1992; Hebbeln et al., 1994; Dokken and Hald, 1996; Weinelt et al., 1996), implying that there must have been a notable water-mass exchange between the Nordic seas and the North Atlantic.

Understanding past environments is a rather challenging task if the region under study has no modern analogues to compare with. The interpretation of the Last Glacial paleoenvironment of the Nordic seas is, in this respect, particularly challenging because it is often hampered by an inconsistency in the downcore occurrence of important proxy tools. For instance, paleoceanographically crucial pelagic microfossil groups are either lacking from the fossil record or are extremely impoverished in species numbers. The bathyal conditions are usually best looked at using benthic forminifera. However, the glacial and interglacial species assemblages of the Nordic seas differ from each other in showing during the glacial interval just a few, mainly infaunal species (e.g., Struck, 1995). This common lack of epibenthic foraminifera in glacial core sections makes it difficult to establish dependable epibenthic δ^{13}C records, and is the main reason why no profound knowledge exists on the glacial-to-Holocene deep-water mass evolution of the Nordic seas. So far, the only existing benthic δ^{13}C records which also covers the entire LGM comes from the southeastern Norwegian Sea and has been used to interpret the water-mass development between the North Atlantic and the Norwegian Sea (Veum et al., 1992). But this core, as well as others most often used for paleoceanographic studies in the Nordic Seas, originates from the western Norwegian-Barents Sea continental margin, a region with hemipelagic sedimentation that has undergone strong depositional changes since the LGM making it more difficult to rule out local depositional effects on the various core records (e.g., Laberg and Vorren, 1995; Bondevik et al., 1997).

In order to overcome, at least partially, the various obstacles associated with sediment records from the Nordic seas and to obtain a constructive paleoceanographic interpretation with a more than regional implication it seems imperative to integrate a multitude of different proxy tools from a ‘pelagic’ core site with reasonably high sedimentation rates but less strong local overprint. By incorporating various benthic and planktic stable isotope and faunal assemblage data as well as lithological records giving evidence of the temporal variations in the input of specific types of iceberg-rafted sediments, an attempt is made in this study to interpret the complex water mass history of the Nordic seas since the final phase of the last glaciation. Besides interpreting the various proxy records from the main investigation area in the central Nordic seas which today is influenced by inflowing Atlantic surface-water and deep-water formation, we will also compare these data with records from a site in the western Fram Strait directly underlying the outflowing polar waters from the Arctic Ocean. This comparison will allow us to interpret not only the glacial-to-interglacial water-mass evolution between the Nordic seas and the North Atlantic but also to relate the observations made in the central Nordic seas with the crucial oceanic changes occurring near the Arctic Ocean gateway.

2. Sites, material, and methods

The main site investigated, PS1243, is located on the eastern flank of the Jan Mayen Ridge at ~2,700 m water depth (Fig. 1). Surface sediments from this area reveal the highest carbonate contents in the Nordic seas (Johannessen et al., 1994), underlining the pelagic nature of this particluar region. In addition, the core position is well suited to trace the various water masses of the Greenland Sea and the Iceland Sea, where the main deep-water formation takes place today, and the Norwegian Sea

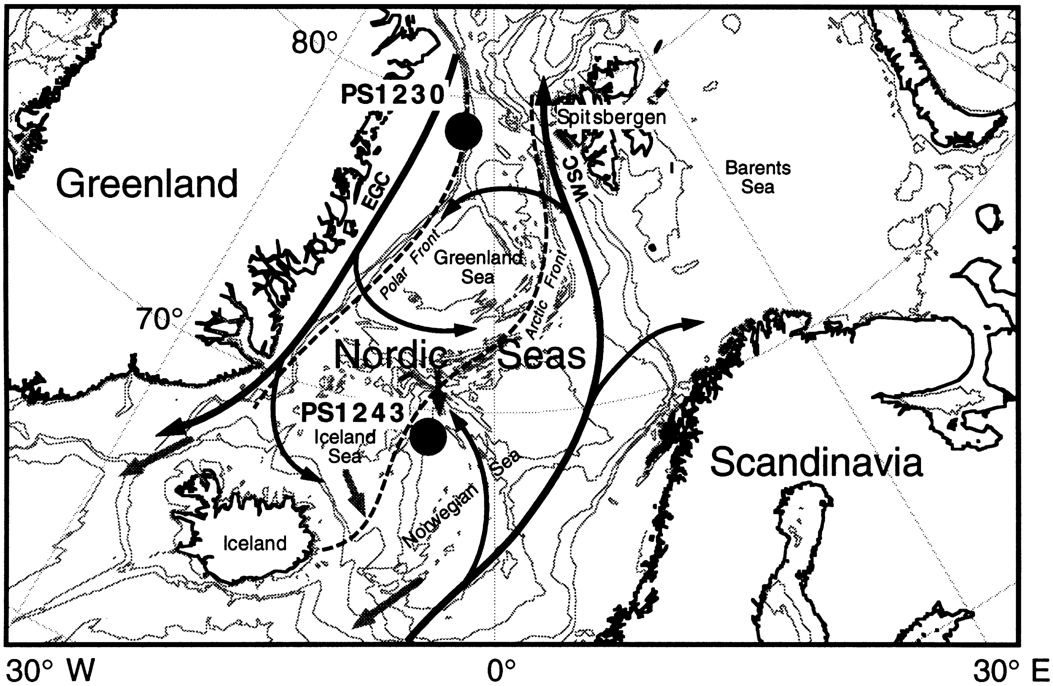

Fig. 1. Present day surface (black arrows) and deep (grey arrows) water circulation in the Norwegian, Greenland, and Iceland seas (Nordic seas). Shown are the two investigated sites and the two dominant oceanographic fronts (Polar and Arctic Fronts) which separate the Nordic seas into different water masses; WSC (West Spitsbergen Current), EGC (East Greenland Current).

which is mostly affected by the warm Atlantic water. Substantial amounts of the deep water leave the Nordic seas southward through the Norwegian Basin. Relatively warm and saline Atlantic surface water flows into the Arctic Ocean through the eastern Fram Strait as West Spitsbergen Current (WSC), whereby water masses from the Arctic Ocean exit in a southward direction along the continental slope of Greenland with the cold East Greenland Current (EGC) being the major component. This difference in water mass flow and properties causes the formation of the two distinctive oceanic fronts, the Polar and Arctic Fronts (Fig. 1).

Sediment samples were taken from core PS1243-1 (core diametre 10 cm) as 1 cm thick slabs at 1 cm intervals. The boxcore PS1243-2 (size $50 \times 50 \times 50$ cm) was usually sampled every 2 cm also as 1 cm thick slabs; additional sampling was carried out with syringes (10 ml) to obtain the dry bulk density of the sediment for calculating accumulation rates. Box core PS1230 was sampled every 1 cm throughout.

Counts of the benthic and planktic foraminiferal assemblages were conducted on two size fractions, 63–125 μm and > 125 μm. This approach was used because previous investigations have shown that changes in test size of the important subpolar planktic species *Turborotalita quinqueloba* is a significant feature in the Nordic seas for the inflow of Atlantic water during the last glaciation (Bauch, 1994; Hebbeln et al., 1994).

The observation and quantification of ice-rafted debris (IRD) in glacial and deglacial marine sediments of the Nordic seas can give an indication of past ice-sheet fluctuations (e.g., Baumann et al., 1995). The IRD composition > 250 μm was carefully studied, providing information on the variability of two dominant lithogenic types: (1) sedimentary rock clasts that are often a greyish, organic-rich siltstone (clastic IRD); (2) crystalline rock fragments (crystalline IRD) of various kind (e.g., mono- and polycrystalline grains of igneous origin and metamorphic rock fragments). There have been numerous attempts to define the provenances of the various IRD types occurring in Nordic seas sediment cores (e.g., Spielhagen 1990; Birgisdottir, 1991; Bischof, 1994). Due to strong similarities in crystalline rock types on the land masses on either side of the Nordic seas, only sedimentary clasts, such as Upper Cretaceous chalk, seem to have provided definite information on the direction of past iceberg drift (Spielhagen, 1991). The occurrence of organic-rich clastic IRD has been noted before in glacial core sections (Bauch et al., 1996; Bischof et al., 1997). It is particularly characteristic within dark layers in cores from the eastern sector of the Nordic seas (Henrich et al., 1989; Bischof, 1994). The origin of these organic-rich material seems to point to the wide and shallow western Eurasian shelves (Wagner and Henrich, 1994). As these sedimentary clasts are a rather conspicuous type of IRD also in other areas of the Nordic seas (Bauch et al., 1996), its particular temporal occurrence may therefore provide important information on glacier ice fluctuation on these northern shelves.

In order to define the possible age and provenance of the clastic IRD, the core section which contained the highest numbers of this rock type was investigated with palynological methods. For this purpose, the sedimentary rock fragments were handpicked and processed. The procedures for processing palynological samples and the further preparation of strewn slides are described in detail by Matthiessen (1995).

Stable isotope analyses were conducted on planktic and benthic foraminifera. The carbon isotopes in the epibenthic-living species *Cibicidoides wuellerstorfi* are known to record the $\delta^{13}C$ of the ambient water (e.g., McCorkle and Keigwin, 1994). Therefore, *C. wuellerstorfi* is often preferred over other species to reconstruct past variations in deep-ocean ventilation, i.e., in nutrients and oxygenation (Sarnthein et al., 1994). Benthic forminiferal $\delta^{18}O$ records usually give the best indication of glacial to interglacial variations in global ice volume, as it is generally assumed that they are less affected by local changes in temperatures and freshwater fluxes than planktic $\delta^{18}O$ values. However, previous benthic $\delta^{18}O$ records from the Nordic seas have revealed some unusually light values for the Last Glacial interval (Duplessy et al., 1988; Veum et al., 1992; Costello and Bauch, 1997). Therefore, stable isotope measurements were performed on two benthic species, the epibenthic species *C. wuellerstorfi* and the shallow-infaunal species *Oridorsalis umbonatus*. Because of the well-known departure from isotopic calcite equilibrium, the $\delta^{18}O$ values of both species were corrected by $+0.64$ and $+0.36‰$ respectively. From the planktic assemblage the polar species *Neogloboquadrina pachyderma* sinistral (sin.) was analyzed. All stable isotope analyses were carried out at the Leibniz Laboratory of Kiel University using the fully automated Kiel Carbonate Preparation Device and a Finnigan MAT 251 mass spectrometre system. The analytical accuracy of this system is $\pm 0.07‰$ for $\delta^{18}O$ and $\pm 0.04‰$ for $\delta^{13}C$ (NBS-19) and all measurements were calibrated to Pee Dee Belemnite (PDB).

Age control of the studied cores is based on AMS ^{14}C dates measured on *N. pachyderma* sin. To be comparative with other paleoceanographic studies, a correction by subtracting 400 yr was made to all radiocarbon ages to account for the ocean inventory age (e.g., Veum et al., 1992; Sarnthein et al., 1995; Voelker et al., 1998). Ages of samples between ^{14}C fixpoints were first obtained by calculating linear sedimentation rates. In a second step, each sample was given a calendar year following Stuiver and Reimers (1993) until 18 ka ^{14}C ka and Bard et al. (1994) for the older core section. If not marked specifically, all ages discussed are given in calendar years BP (cal. kyr).

At site PS1243, both cores contained a 2 cm thick ash layer comprised of transparent glass shards. We took advantage of this discrete ash layer to splice together boxcore PS1243-2 and its undisturbed surface layer with the section from below this horizon which originates from gravity core PS1243-1.

3. Sedimentation rates

The stratigraphic record of composite core PS1243 extends back to 30 cal. kyr (Figs. 2 and 3), covering the time since the end of OIS 3. The radiocarbon age/depth relation reveals that sedimentation rates varied between 1 and 6.5 cm/kyr, with highest sedimentation rates being observed between 14 and 6 cal. kyr. The time span represented by each of the 1 cm thick sample slabs averages ~ 550 kyr for the time 30–16 cal. kyr, ~ 220 yr between 14 and 6 cal. kyr, and ~ 340 yr for the last 6 cal. kyr.

As revealed by X-ray photography (Birgisdottir, 1991), the investigated composite core section is an undisturbed sediment sequence. The glacial and deglacial sediment is mainly a silty clay with a sand-size components that varies between 6 and 24% (Birgisdottir, 1991). Above 32 cm core depth the sediment turns into a foraminiferal ooze showing a bulk carbonate content (wt %) of up to $\sim 50\%$ (Bauch et al., 2000a). This increase in carbonate content indicates the typical change from a glacial, hemi-pelagic to a dominantly pelagic depositional setting. The prominent ash layer noted at 44.5 cm depth in core PS1243 is identified as Vedde Ash (Fig. 3). This is confirmed by the radiocarbon date from just below the ash, which yielded an uncorrected age of 10.63 ka ^{14}C BP ± 150 yr, and by geochemical analyses of the ash particles themselves (H.-J. Wallrabe-Adams pers. com. 1998). The purity of the layer with regard to glass-shard content, its well-defined base, and the lack of any signs of

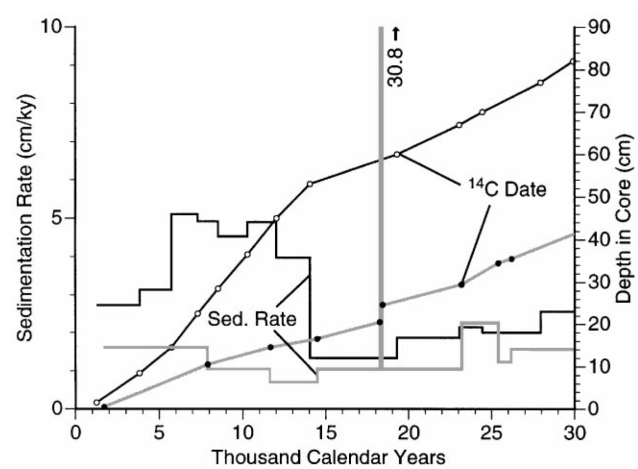

Fig. 2. Linear sedimentation rates and age/depth relation of cores PS1243 (black lines) and PS1230 (grey lines). The age/depth relation is based on calendar years (see also Fig. 3).

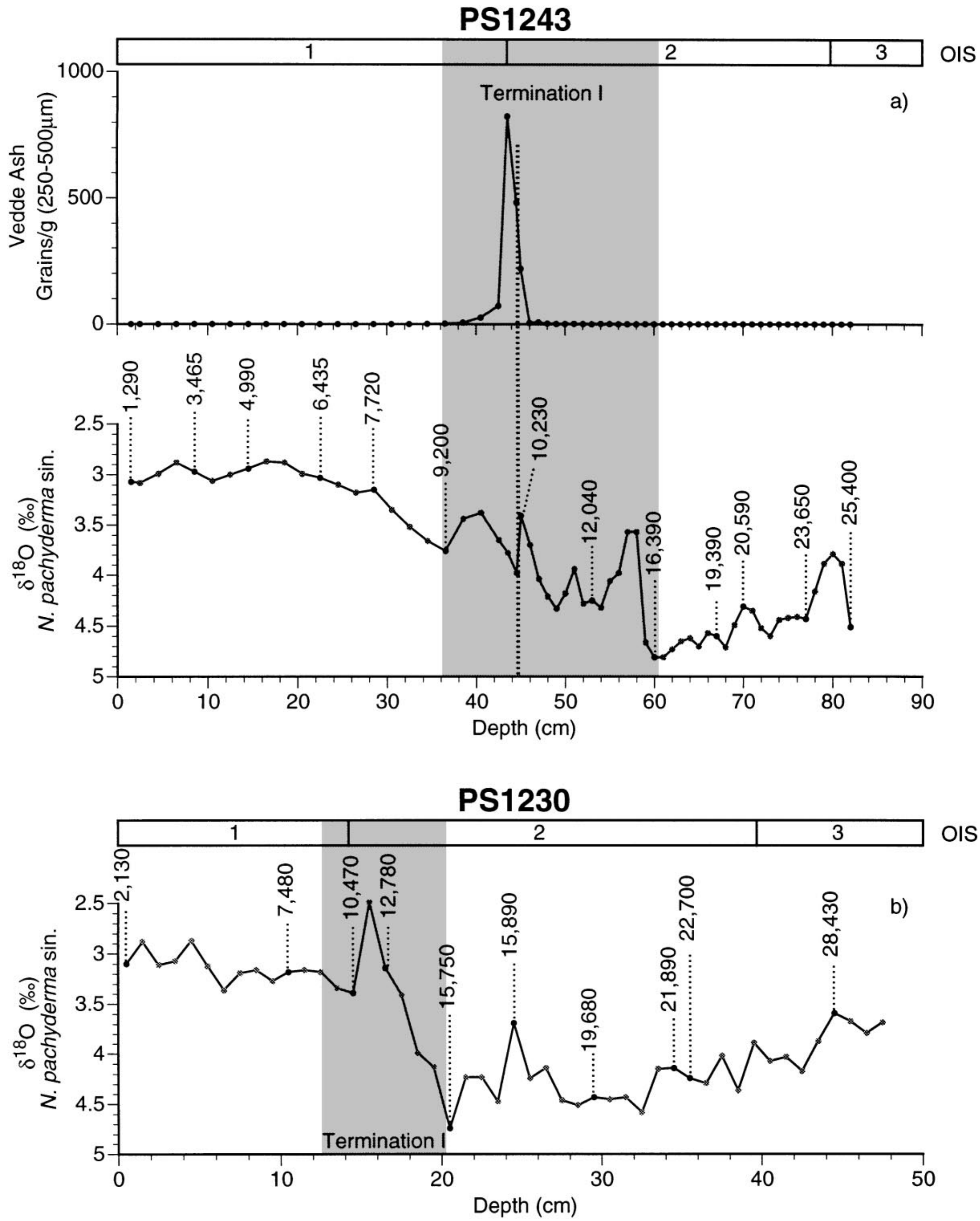

Fig. 3. Planktic oxygen isotope records of the polar species *Neogloboquadrina pachyderma* sinistral in cores PS1243 and PS1230. Stippled line in PS1243 denotes the basis of the Vedde Ash layer. All radiocarbon dates (conventional ^{14}C-yr) shown were reservoir corrected by subtracting 400 yr.

bioturbations in the X-rays all imply that the tephra was deposited rapidly after eruption.

Sedimentation rates in core PS1230 from the western Fram Strait are considerably less high than in PS1243, varying between 1 and 2 cm/kyr for most of the investigated time interval (Fig. 2). The glacial and deglacial sediment at this site is largely comprised of a sandy-silty clay of which the sand content makes up between 20 and 50%. In the Holocene part above $\sim$ 13 cm core depth, the sand contents decreases usually below 10% (Spielhagen, 1990). The carbonate content in the lower, glacial core interval ranges between 4 and 9%, mostly of which is of detrital origin, whereas the Holocene part shows rather constant values between 3 and 5% (Spielhagen, 1991). As can be realized from the reduced sedimentation rates in core PS1230, the low modern carbonate content seems primarily a reflection of the strong perennial ice coverage at the site and, hence, low carbonate bioproductivity in these polar waters rather than a result of sediment dilution despite the proximity of this site to the Greenland margin. However, increasing corrosion and fragmentation of foraminiferal test was noticed above 13 cm core depth, an observation that could have additionally affected the total carbonate contents.

4. Records from the central Nordic seas

4.1. Iceberg-rafted debris (IRD)

The IRD records for the past 30 cal. kyr illustrates that ice rafting was relatively low until 26 cal. kyr BP (Fig. 4). The following strong increase in IRD (26–18 cal. kyr) remained on a high level throughout OIS 2, i.e., the phase with maximum extent of the Weichselian ice sheets. Afterwards, IRD concentrations never regained the high glacial values. Nevertheless, there are two more notable spikes centred at 14 and at 12–13 cal. kyr until IRD deposition eventually ceased at 10 cal. kyr. The ensuing part of the Holocene section is devoid of any significant IRD, although, in the topmost sample there is a slight recurrence of IRD. The two samples which essentially cover the Vedde Ash layer ($\sim$ 12 cal. kyr) do not contain any IRD but only glass shards and a few biogenic components, corroborating the inference made above of its rapid deposition.

Each of the two main IRD components reveal a different pattern between 26 and 22 and between 15 and 13 cal. kyr and it seems as if both IRD records are anti-correlated. The clastic IRD record reveals major spikes centered at 23 and 14 cal. kyr. In time, the elder of the two spikes correlates well with the occurrence of ice-rafting event H2 in the North Atlantic (Bond et al., 1993). Although different types of grey, organic-rich sedimentary clasts occur in glacial sediments of the Nordic seas (Wagner and Henrich, 1994), in the core section dealt with here the clastic IRD is composed of medium grey colour and appears to be all of the same kind. In order to learn more about age and provenance of these sedimentary clasts the two samples from the spike around 23 cal. kyr were selected for palynological studies. The results revealed *Batioladinium sp*., a dinoflagellate genus with restricted stratigraphic range described from Greenland in mudstones/sandstones of Lower Cretaceous age (Nähr-Hagen, 1993). Around the Nordic seas, rock types of this age cover large areas of the Barents Sea shelf region, but are found only very localized on the East Greenland shelf (Okulitch et al., 1989).

4.2. Planktic and benthic foraminferal assemblages

Of the faunal assemblage data only those species are shown which have been identified before to provide crucial paleoceanographic information (Figs. 4c and d). During the climatic change from a glacial to an interglacial mode *C. wuellerstorfi*, a foraminifer typically representing interglacial water-mass conditions in the Nordic seas, becomes the dominant benthic species (Belanger, 1982; Struck, 1995). Glacial sediments from the Nordic seas contain only few deep-sea species, e.g. *O. umbonatus*, and these usually in comparatively low numbers (Struck, 1995). But Last Glacial sediments from the Nordic seas also typically reveal *Siphotextularia rolshauseni*, an infaunal species which can be used as a stratigraphic marker for OIS 2 (Nees and Struck, 1994; Struck, 1995). The abundance record of this species in core PS1243 (Fig. 4d), extending between 28 and 17 cal. kyr and disappearing at the onset of deglaciation, clearly underlines the previous studies on its stratigraphic occurrence. Since *S. rolshauseni* does not live in the Nordic seas today, nothing is known about its past environmental preferences or why it became so widely dispersed here during OIS 2. In contrast to *C. wuellerstorfi*, which becomes more abundant only after 12 cal. kyr, the temporally confined occurrence of *S. rolshauseni* may imply that very special conditions prevailed in the Nordic seas during the final phase of the last glaciation.

Among the planktic foraminifera, *N. pachyderma* sin. is commonly accepted as the only species reflecting polar surface water and glacial conditions. In large areas of the Nordic seas, Holocene sediments reveal that *N. pachyderma* sin. and *Turborotalita quinqueloba* are the two dominant species of the planktic foraminiferal assemblage (Kellogg, 1984; Bauch et al., 1996). In core PS1243, the relative abundance of *T. quinqueloba*, which is nearly inversely related to *N. pachyderma* sin (%), increases up to 75% (within the size class > 125 μm) during the mid-Holocene and remains above 50% between 9 and 4 cal. kyr (Bauch, 1997).

The records of *T. quinqueloba* reveal only in the size-class 63–125 μm an abundant occurrence between 28 and 18 cal. kyr (Fig. 4c). During the early deglaciation (18–14 cal. kyr), however, the two different test-size records of *T. quinqueloba* show a significant increase between 14 and 13 cal. kyr, probably coeval in time with the Bølling/Allerød warming in this area (Koç-Karpuz and Jansen, 1992). In the size-class > 125 μm, polar species abundance dropped by 40% during this event. After a renewed return to more polar conditions between 13 and 12 cal. kyr, the relative number of *N. pachyderma* sin. strongly decreases after 12 cal. kyr, reaching lowest values

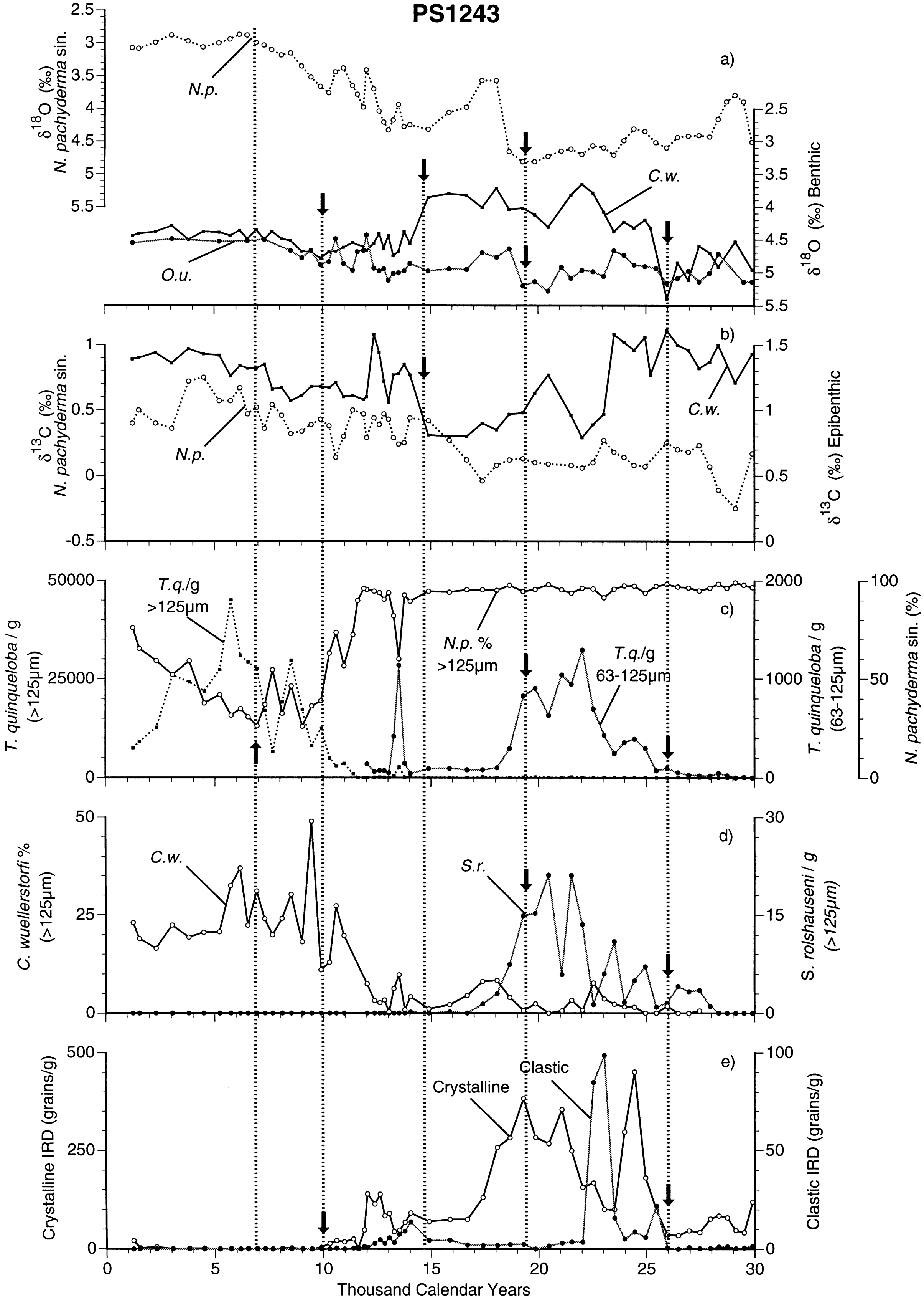

Fig. 4. Comparison of downcore records from the Norwegian Basin with arrows indicating major points of change in the various records. (a) $\delta^{18}O$ records of the polar species *Neogloboquadrina pachyderma* sin. (*N.p.*) and the two benthic foraminifera *Cibicidoides wuellerstorfi* (*C.w.*) and *Oridorsalis umbonatus* (*O.u.*). (b) $\delta^{13}C$ records of *N.p.* and *C.w.*. (c) Test concentrations (per gram sediment) and relative abundances (%) of planktic foraminifera from different size classes. (d) Benthic foraminiferal test concentrations of *Siphotextularia rolshauseni* (*S.r.*) in comparison with the relative abundance *C. wuellerstorfi*. (e) Grain concentration of two different groups of iceberg-rafted rock debris, clastic and crystalline IRD.

at 9 and at 7 cal. kyr. Noteworthy are two events centred around 10.5 and 8 cal. kyr when polar species abundance increased. After $\sim$ 7 cal. kyr, *N. pachyderma* sin. started to become the dominant species again.

When comparing all faunal records in Fig. 4, two major points are striking: (1) during the glacial part the appearance of small-sized *T. quinqueloba* and *S. rolshauseni* are of similar duration; (2) both the relative abundance of *C. wuellerstorfi* and total supolar fauna test concentrations steeply increased after 12 cal. kyr, although the former does not show the marked decrease in tests numbers as noted for the subpolar species after 7 cal. kyr when polar surface conditions gradually became dominant again.

4.3. Carbon and oxygen isotope records

The main excursions in the planktic $\delta^{13}C$ and $\delta^{18}O$ isotope records always occur at the same time during the glacial and deglacial part (Fig. 4a and b). This is particularly noticeable at 29 cal. kyr, and around 17–18 and 10–11 cal. kyr when changes of up to 0.5‰ in $\delta^{13}C$ are recorded. Carbon isotope values during the glacial section are significantly more depleted (down to -0.3‰) than during the ensuing deglaciation when they fluctuate on a higher level, mainly between 0.2 and 0.5‰. Highest Holocene $\delta^{13}C$ values of about 0.8‰ were eventually reached around 4 cal. kyr. This maximum in planktic $\delta^{13}C$ values and its significant drop after 4 cal. kyr seems a very distinctive feature as it is also observable in other sediment cores from the eastern Norwegian Sea mainly (Bauch and Weinelt, 1997).

The epibenthic $\delta^{13}C$ record (Fig. 4b) can be roughly subdivided into several, from each other distinctly different intervals. Nearly highest $\delta^{13}C$ values are observed before $\sim$ 23 cal. kyr whereas the interval between 23 and 15 cal. kyr is marked by two major depletions. Although $\delta^{13}C$ values never drop back to the low level observed at 15 cal. kyr, the $\delta^{13}C$ record remains rather variable between 15 and 8 cal. kyr, revealing changes of more than 0.5‰. After 8 cal. kyr benthic $\delta^{13}C$ values increased until late Holocene values of about 1.4‰ were first reached at $\sim$ 5 cal. kyr.

All three oxygen records correspond quite well during the early part of the glacial interval, reaching a preliminary trough with high $\delta^{18}O$ values at 22 cal. kyr and a significant decrease near 20 cal. kyr (Fig. 4a). But whereas *O. umbonatus* and *N. pachyderma* sin. oxygen values further increase during the remaining part of OIS 2, the epibenthic $\delta^{18}O$ record is opposite, revealing comparatively low values. At 2700 m water depth $\delta^{18}O$ values in *C. wuellerstorfi* should be expected comparable to those from the North Atlantic region where highest values are usually found towards the end of the LGM, before deglaciation started at about 18 cal. kyr (Sarnthein et al., 1994). Our glacial epibenthic $\delta^{18}O$ values are also significantly more depleted than previously published data from the southeastern Norwegian Sea (Veum et al., 1992).

The endobenthic record of *O. umbonatus*, on the other hand, runs more or less parallel with the record of *N. pachyderma* sin. (Fig. 4a), showing the highest values around 21–19 cal. kyr. However, because of its shallow endobenthic habitat (Corliss, 1985) some specimens of *O. umbonatus* may be slightly younger than their actual stratigraphical position would indicate. For instance, this may be the case for the slight offset noted in the timing of highest glacial $\delta^{18}O$ values in *N. pachyderma* sin. and *O. umbonatus* which occurred during times of lowest sedimentation rates in core PS1243 (Fig. 2).

The general good parallelism in the $\delta^{18}O$ records of *N. pachyderma* sin. and *O. umbonatus* is also recognized during the first part of the deglaciation when both records suddenly drop to significantly lower values between 19 and 17 cal. kyr. In *C. wuellerstorfi* the increasing trend in the $\delta^{18}O$ record after 15 cal. kyr persisted until 10 cal. kyr. This $\delta^{18}O$ increase during deglaciation is certainly contrary to the postglacial global sea-level record which reveals only a steady rise but never a notable fall (Fairbanks, 1989).

Taking into account all records from core PS1243, we are able to derive from them several major turning points (arrows in in Fig. 4). The first is noted at about 26 cal. kyr when a sudden increase of IRD deposition is coincident with high oxygen values in all three $\delta^{18}O$ records, and an increase in abundance of small-sized *T. quinqueloba* roughly synchronous with the appearance of *S. rolshauseni*. A second major change occurred close to 19 cal. kyr. At this time, $\delta^{18}O$ values of *O. umbonatus* and *N. pachyderma* sin. decreased, time coeval with receding IRD and test concentrations of *T. quinqueloba* and *S. rolshauseni*. A third transition is the steep increase of $\delta^{18}O$ values in *C. wuellerstorfi* after 15 cal. kyr which, in its terminating trough near 13.5 cal. kyr, is synchronous with a notable surface warming, an increase of subpolar and *C. wuellerstorfi* abundance as well as an intermittent reduction in IRD deposition. The next major change is noted at about 10 cal. kyr when IRD input to site PS1243 had completely stopped. This was also the time when the two benthic $\delta^{18}O$ records finally converged onto the same value level where they roughly remained since. The last two major points of change are observed at about 7 cal. kyr when polar species abundance began to increase and at 5 cal. kyr when epibenthic $\delta^{13}C$ values had come to a consistent level.

5. Records in the western Fram Strait

Unlike PS1243, which may in large reflect oceanographic changes in the central and southern Nordic seas directly induced by variations in the intensity of inflowing Atlantic water masses, the site in the Fram Strait may

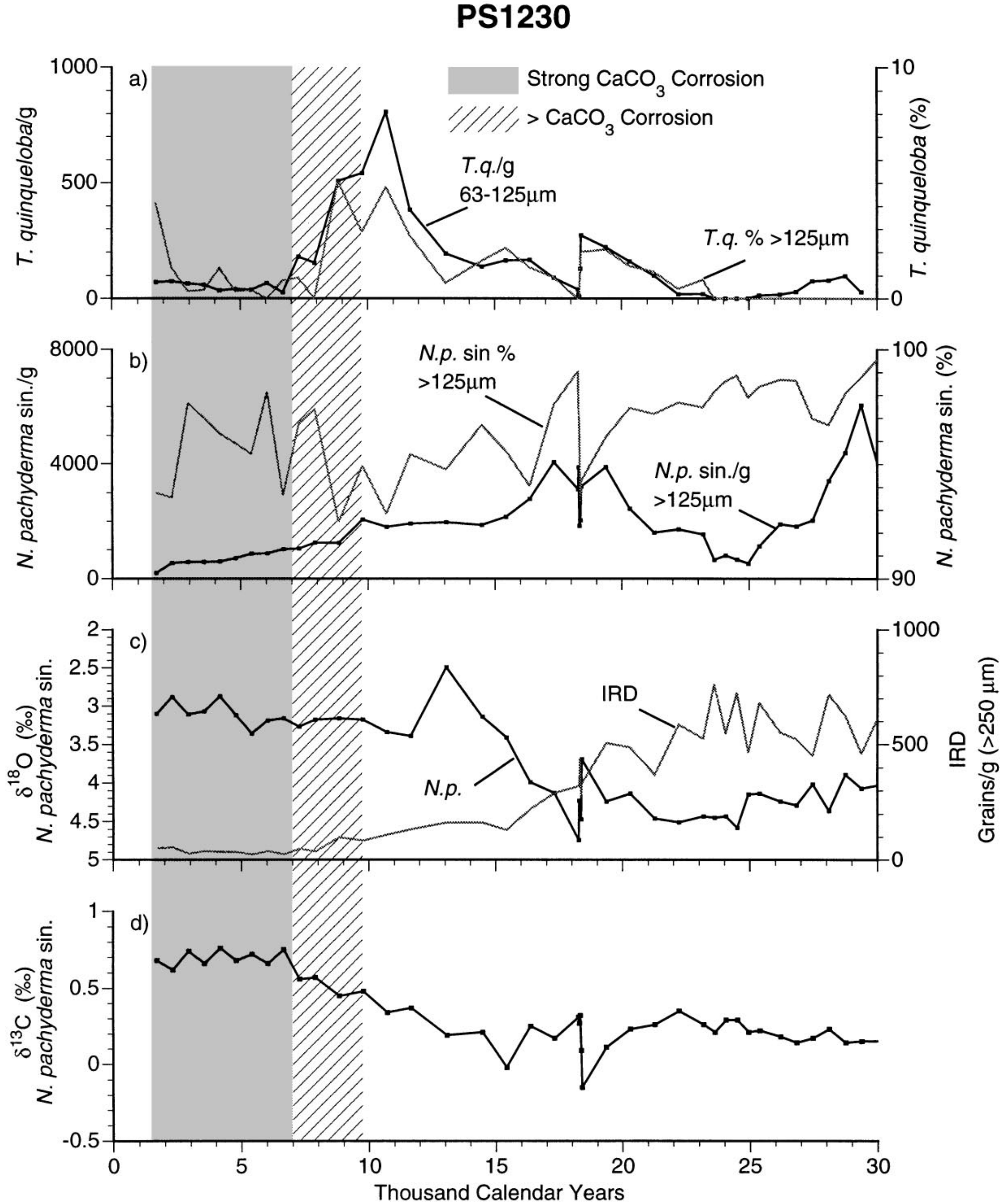

Fig. 5. Distribution of faunal, lithological, and isotopic proxy data from the western Fram Strait during the past 30 cal. kyr.

be suited to investigate the complex oceanographic regime in the high Arctic region (Fig. 5). On the basis of the calendar year chronology the oxygen isotope record of *N. pachyderma* sin. marks highest glacial $\delta^{18}O$ values of about 4.8‰ at $\sim$ 18 cal. kyr which is comparable with the results in core PS1243. However, in core PS1230 a significant depletion is observed just prior to this $\delta^{18}O$ maximum, centred at $\sim$ 18.5 cal. kyr. This event is also identifiable in planktic $\delta^{18}O$ records from much further south on the western Iceland Plateau (Bauch, 1994; Koç and Jansen, 1994), and may have been induced by oceanographic changes occurring at the Greenland ice margin, because a similar event is not recognizable in sediment cores from the eastern Fram Strait and the Norwegian Sea (Jones and Keigwin, 1988; Weinelt et al., 1991). Caused by the commencing deglaciation after 18 cal. kyr, the decreasing $\delta^{18}O$ values are accompanied by a continuous increase in $\delta^{13}C$. The latter eventually reached a constistent level of about 0.7‰ at 7 cal. kyr.

Although no lithological distinction was made between rock types in core PS1230, the record of total IRD deposition is very much comparable to core PS1243. The glacial section is characterized by highest amounts of IRD until about 19 cal. kyr whereas lowest values are found during most of the Holocene, after about 10 cal. kyr.

The small-sized test record of *T. quinqueloba* reveals the occurrence of some specimens centred around 28 cal. kyr. A second more pronounced increase in subpolar species occurred after 23 cal. kyr and abruptly terminated at 18.5 cal. kyr. Similar ages for the occurrence of small-sized *T. quinqueloba* have been also reported from records of the southeastern Fram Strait (Hebbeln et al., 1994) and are quite consistent with the findings noted in the glacial interval of PS1243. Comparing the Holocene record, however, it is intriguing that in the Fram Strait subpolar foraminiferal abundance seems highest between 11 and 9 cal. kyr (Hald et al., 1996). This is at first hard to reconcile with our data from core PS1243, considering that the latter core is positioned upstream showing the subpolar maximum between 10 and 6 cal. kyr. However, we have observed increasing foraminiferal test corrosion in PS1230 after 9 cal. kyr, becoming even more severe after 7 cal. kyr, when test fragmentation is very common. Therefore, partial dissolution must be regarded responsible for the low test concentrations in core PS1230 during this time. Furthermore, due to differential dissolution effects among the two species an increase in calcite solubility after 9 cal. kyr must have strongly affected the relative species composition, most likely causing an apparently higher proportions of the less-calcified species *T. quinqueloba* in the Fram Strait during the early Holocene. This assumption gains further support from plankton tow studies in this region which reveal considerably higher proportions of *T. quinqueloba* in the water column (Carstens et al., 1997) than in the underlying upper Holocene sediments. Interestingly, the onset of severe test corrosion at 7 cal. kyr is time coeval with high values in planktic $\delta^{13}C$.

6. Paleoceanographic reconstruction and climatic implications

6.1. Last Glaciation

Distinct IRD events, recognized in the North Atlantic as 'Heinrich' layers during distinct cold phase of the Last Glaciation, are interpreted as the result of massive iceberg discharges due to ice-sheet growth over North America - Greenland and Scandinavia (Bond et al., 1993; Fronval et al., 1995). Whether these ice sheets expanded synchronously is a matter of methodology and precision of core chronologies (Dowdeswell et al., 1999), but seems not so relevant for the Nordic seas as this region was always dominantly influenced by the fluctuations of the western Scandinavian ice sheets (Baumann et al., 1995). The mechanism for ice-sheet growth on Scandinavia seems simple as it depends on summer air temperatures that are cold enough to prevent an excess of summer melt over winter snow precipitation. A substantial amount of the moisture transferred to western Scandinavia originates from evaporation in the low-latitude North Atlantic. Therefore, past variations in the size of the Scandinavian ice sheet were directly depending on the flux rate of oceanic–atmospheric heat and moisture towards high-northern latitudes (cf. Hebbeln et al., 1994) which, besides sea-level changes, also controlled the rate in iceberg calving. Because melting of icebergs can only occur when the ambient water and/or the air temperature is above 0°C, the recognition of IRD in glacial sediments of the Nordic seas implies that icebergs were actually melting away thereby releasing both incorporated rock fragments and relatively cold freshwater. This thought may be a trivial conception if applied for the mid-latitude North Atlantic where icebergs were drifting southward into relatively warmer latitudes. As it is generally believed that the glacial Nordic seas were cold and covered by sea ice, pack ice, and icebergs for most year around except the summer season, the occurrence of highest IRD during the glacial interval could also mean that the water temperatures at this time were considerable warmer than thought previously.

The increase in flux rates of IRD at about 26–24 cal. kyr (Fig. 6) indicates that the balance between ice growth and sea-level fall around the Nordic seas had reached a critical point, causing enhanced discharge of icebergs near the shelf edge. This interpretation is in accordance with studies from the western Barents Sea (Elverhøi et al., 1995; Vorren and Laberg, 1996). The relatively high input of clastic IRD of lower Cretaceous age at site PS1243 points to the Barents Sea shelf and its archipelagos (Barents shelf region) as the principle source area (Elverhøi et al., 1995; Bischof et al., 1997). The age of the two clastic IRD spikes (25.5 and 23 cal. kyr) is in good agreement with newly published data that show increased transportation of organic-rich terrigenous material off the northwestern Barents Sea shelf into the deeper Arctic basin at the same time (Knies and Stein, 1998). Because global sea level was still falling during this time, it seems evident that these two spikes in IRD reflect major ice growth/surging in the Barents shelf region which also led to the increased transfer of clastic IRD off the shelf and into the central Nordic seas via iceberg rafting.

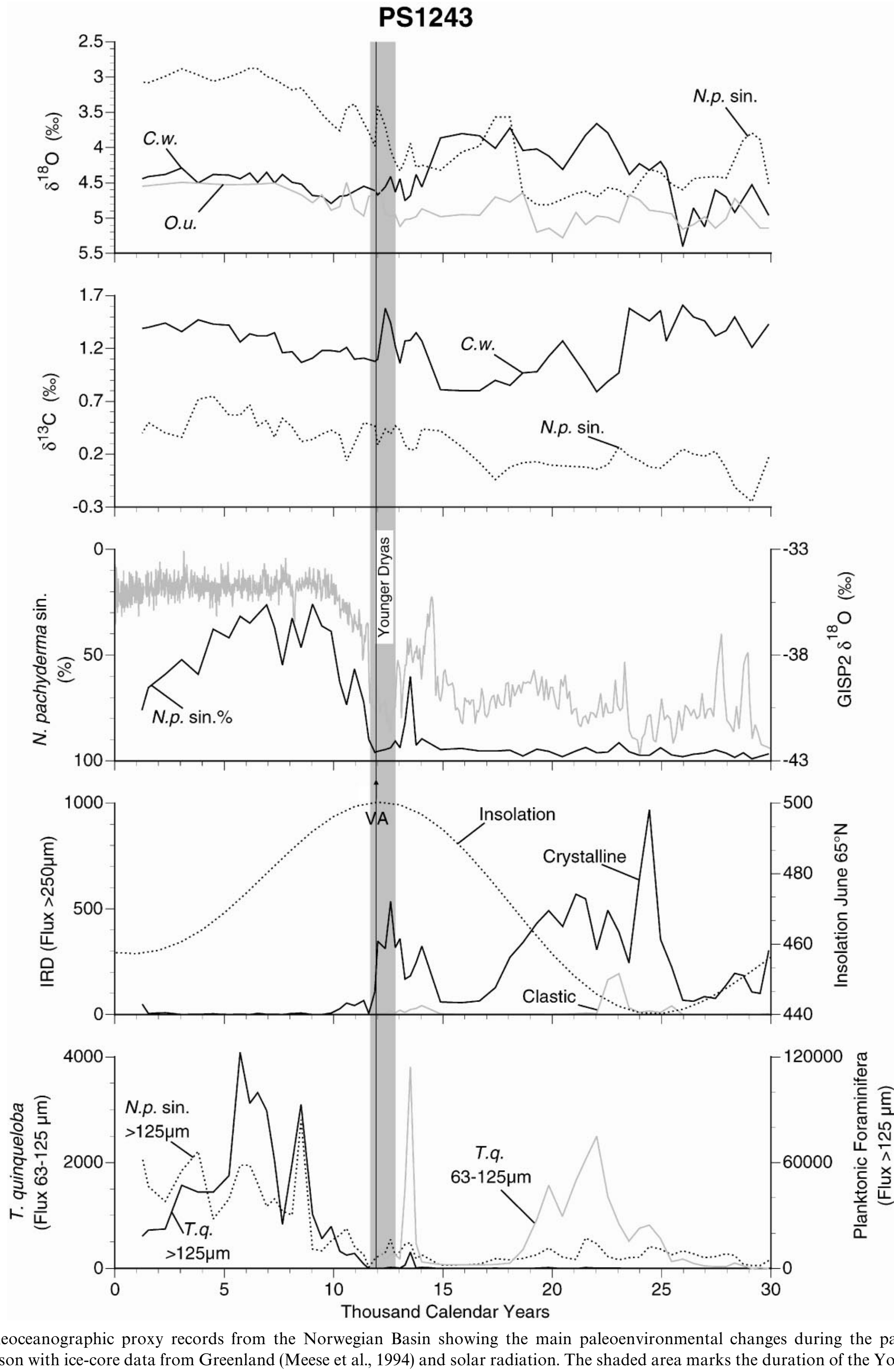

Fig. 6. Paleoceanographic proxy records from the Norwegian Basin showing the main paleoenvironmental changes during the past 30 cal. yr in comparison with ice-core data from Greenland (Meese et al., 1994) and solar radiation. The shaded area marks the duration of the Younger Dryas cold event. The thin line represents the base of the Vedde Ash (VA). Flux rates of foraminifera and IRD are expressed as number of grains*cm^{-2}*kyr^{-1}.

The constantly high input of crystalline rock fragments between 22 and 19 cal. kyr indicates that the ice-sheet margins around the Nordic seas remained active in terms of iceberg production. However, the distinctive lack of clastic IRD during this time, could either imply that the sediment clasts were only incorporated into the ice during times of significant ice growth in specific areas or that iceberg drift had changed direction. The occurrence of high numbers of small-sized *T. quinqueloba* in the Norwegian Basin and the Fram Strait while global ice volume was reaching its maximum may indeed indicate a northward flow of air and water masses which would explain the lack of clastic IRD at his time due to a change in the pathway of icebergs.

The occurrence of subpolar foraminifera alongside with increasing $\delta^{18}O$ values (*N. pachyderma* sin. and *O. umbonatus*) was previously interpreted as evidence for seasonally open waters in the Nordic seas during the LGM (Bauch, 1994; Weinelt et al., 1996). There could be little doubt that the surface-water conditions during this time were somehow associated with inflowing Atlantic water and that this situation must have had a positive feedback on the ice-sheet growth over the Barents Sea region (Hebbeln et al., 1994). The inference of summer sea-ice melting and, thus, open waters in the Nordic seas during the LGM may be further corroborated by the observation of high fluxes of IRD in our central Nordic sea core. For analogy, in the central Arctic Ocean were sea-ice coverage today is close to 100% with relatively little seasonal melting, sediment cores reveal characteristically low fluxes of IRD for the LGM (Nørgaard-Pedersen et al., 1998). The reason for this was probably not the lack of icebergs in the Arctic Ocean during the LGM but rather a cold (below °C) and thick (several 100s m) halocline as today (Bauch et al., 2000b). On the other hand, to interpret the presence of nannoplankton and increased amounts of planktic foraminifera per gram in Last Glacial sediments of the northern Nordic seas as high surface bioproductivity and, thus, open-water conditions per se (Hebbeln et al., 1994; Dokken and Hald, 1996) must be regarded with some caution. Coccoliths and relatively high numbers of foraminifera per gram are also found in Holocene sediments from the perennially ice-covered interior Arctic Ocean (Gard, 1993; Nørgaard-Pedersen et al., 1998; Bauch, 1999), but merely as the result of generally low sedimentation rates, i.e., little accumulation of terrigeneous sediments.

Conceivably, our various faunal and lithological records from the main glacial interval (26–19 cal. kyr) represent conditions which are certainly difficult to explain using the concept of a modern water-mass circulation. In this respect, it is intriguing to see the major change in the faunal and IRD records at 26 cal. kyr to coincide with the sudden decrease in the $\delta^{18}O$ record of *C. wuellerstorfi*. Because these epibenthic $\delta^{18}O$ values are contrary to those found in the North Atlantic for the same time, previous and recent studies have interpreted such low benthic $\delta^{18}O$ excursions in association with low planktic $\delta^{18}O$ values by invoking brine formation (Veum et al., 1992; Vidal et al., 1998; Dokken and Jansen, 1999) whereas others, using benthic faunal evidence (Rasmussen et al., 1996), link them to an inflow of intermediate water.

Plankton trap data from the western Fram Strait show that *T. quinqueloba* lives here within Atlantic waters that becomes advected below the cold and low-saline polar surface waters (Carstens et al., 1997). Such a modern oceanographic setting can be used to help explain the existence of *T. quinqueloba* during the LGM in that relatively warm Atlantic surface waters became subducted below a colder, and due to meltwater, low density and strongly stratified upper surface layer (Fig. 7). Because sea-ice cover not only prevents heat release to the atmosphere but also supports surface water stratification, the unusual low epibenthic $\delta^{18}O$ values in the glacial interval may be partly the result of a gradual warming of the deeper water as is observed in the Greenland Sea today (Budéus et al., 1998). The glacial oceanographic scenario (Fig. 7) would be similar to the modern situation north of Spitsbergen where relatively warm Atlantic surface water (~ 2–4°C) is being subducted underneath the cold Arctic halocline (~ − 1.7°C) causing an inverse temperature relation between the surface water and the underlying intermediate water (Environmental Working Group, 1998). As it can be assumed that the upper water structure in the glacial Nordic seas was of lower salinity than the North Atlantic, deep-water warming could have been enhanced by the downflow of incoming upper Atlantic water along inclined isopycnals and a reduction in vertical convection processes. Another piece of evidence regarding the possible subduction of Atlantic surface water during the last glaciation comes from a high-resolution core from the Denmark Strait. In this core, benthic foraminifera often yielded significantly younger radiocarbon ages than planktic foraminifera (Voelker et al., 1998). These younger ages in the bottom waters might have been caused by the inflow and subduction of upper Atlantic water which had a relatively smaller ^{14}C reservoir age than the meltwater and ice cover stricken surface waters in the Nordic seas.

For the glacial Nordic seas it can be assumed that the ice sheets, which extended onto shallow areas such as the Barents Sea shelf, also existed at least partly in form of ice shelves (Svendsen et al., 1999). As it can be further assumed, katabatic winds were blowing away constantly from the ice-sheet margins towards the ice-covered sea probably creating the formation of open waters (polynyas). These polynyas constituted potential areas of increased sea-ice and dense-water production (Fig. 7). It seems unlikely that dense water production due to sea-ice formation (the so-called brines) was the mechanism responsible for the observed low epibenthic $\delta^{18}O$ values because of the great water depth of our core which would

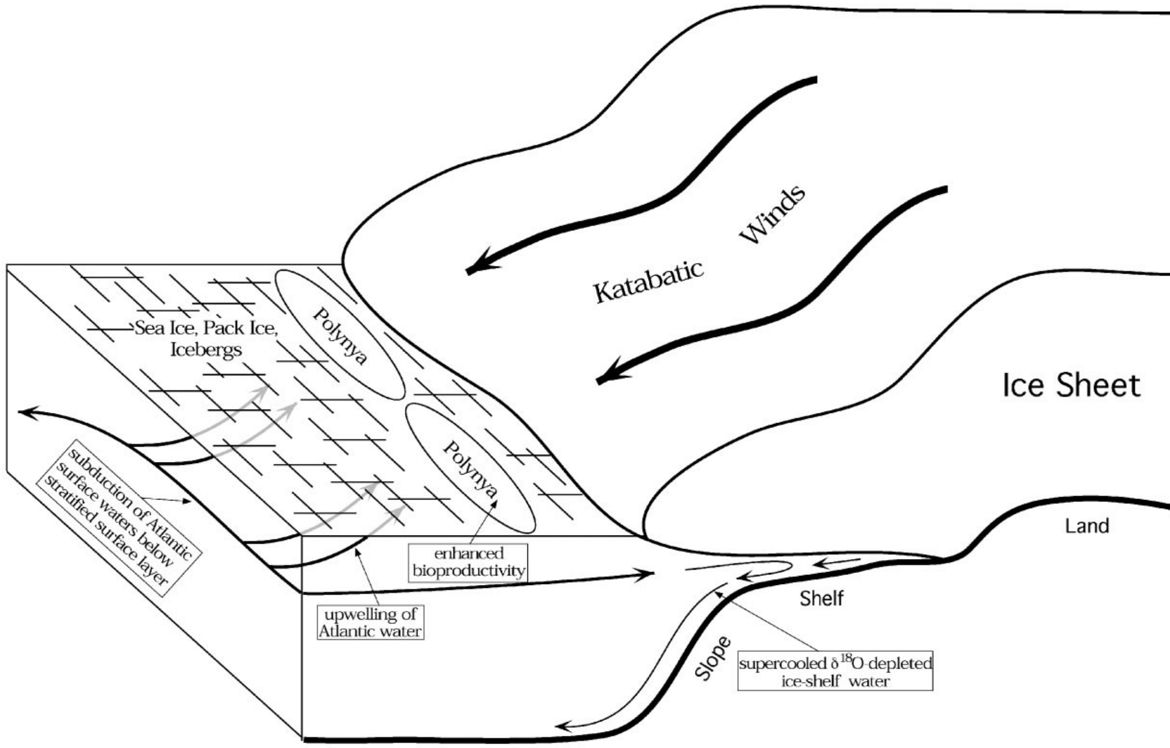

Fig. 7. Schematic drawing of the LGM scenario (ca. 26–18 cal. kyr) in the Nordic seas.

have led to the dilution of the low δ^{18}O signature of the surface water via mixing. Moreover, core PS1243 is located far away from the continental areas, also ruling out brines formed on the continental shelves, as suggested by Dokken and Jansen (1999). Our polynya scenario, however, would have facilitated upwelling, a process which then could have accomodated both, increased surface bioproductivity as well as the advection of comparatively warm and saline water from the North Atlantic. Therefore, the polynya scenario shown in Fig. 7 is suggested by us as a main mechanism that had a strong effect on the environmental conditions in the Nordic seas during the LGM. However, we do not rule out the possible impact of glacier ice also on deep water δ^{18}O. As studies in Antartica have shown supercooling processes at the underside of an ice shelf/ice margin can indeed lead to a noticeable density increase of δ^{18}O depleted, low-salinity surface waters (Foldvik and Gammelsrød, 1988). Since during the LGM deep-water benthic δ^{18}O values from the North Atlantic were about 1‰ higher than in the Nordic seas, the epibenthic δ^{18}O values found in PS1243 would imply about 4°C warmer deep-water temperatures, if all the isotopic change were due to temperature alone. However, such a drastic increase in bottom-water temperature seems unlikely with our present understanding of the physical oceanography during the LGM. Therefore, it remains unanswered which of the two factors, deep-water temperature increase through the advection and subduction of warm Atlantic water or a drawdown of δ^{18}O-depleted, supercooled and/or brine-affected surface waters had the greater effect on our epibenthic foraminiferal δ^{18}O record.

Contrary to the record shown by Veum et al. (1992) from the southwestern Norwegian continental slope, our glacial record of benthic foraminiferal δ^{13}C is very reminiscent of the isotopic trend found in the North Atlantic for similar water depths (Sarnthein et al., 1994), indicating a deep-water link between both regions. That deep water was formed in the Nordic seas during the glacial phase may be inferred from the generally higher δ^{13}C values observed in the Nordic seas compared with the North Atlantic. This is also true for the time interval prior to 23 cal. kyr which reveals particularly high benthic δ^{13}C values in the Nordic seas. However, an overall decrease onto a lower level is observed in the benthic δ^{13}C after $\sim$23 cal. kyr indicating that deep-water conditions during the LGM period differed from the times before. It is interesting to remark that at the same time when insolation began to increase air temperatures over Greenland rose too, indicating that atmospheric conditions at high-northern latitudes underwent an irreversible change towards an interglacial climatic mode (Fig. 6). Because δ^{18}O values (*O.u.* and *N.p.*), i.e., global ice volume, continued to increase for another 4 ky (until $\sim$19 cal. kyr), the generally high flux rates of IRD observed prior to this time were the consequence of enhanced ice sheet/glacier growth around the Nordic seas due to increased precipitation probably forced by this earlier change in atmospheric temperature. As the resulting increase in the production of icebergs and their subsequent melting must have had an effect on the water-mass structure (Maslin et al., 1995; Zahn et al., 1997), the significant $\delta^{13}C$ depletions found, e.g., at ~ 22 cal. kyr (time-coeval with H2), can be taken as evidence for a notable reduction in deep-water formation in the Nordic seas.

Crucial for our interpretation of the particular oceanic conditions during the LGM is also a better understanding of the circumstances which caused the $\delta^{18}O$ difference between the epibenthic-living *C. wuellerstorfi* and the shallow-infaunal species *O. umbonatus*. One argument to produce such two different records could be bioturbational downmixing of tests of *C. wuellerstorfi* from the core section where all three species, *C. wuellerstorfi*, *O. umbonatus*, *N. pachyderma* show a time-coeval $\delta^{18}O$ depletion (between 19 and 17 cal. kyr). Prior to this, however, a $\delta^{18}O$ increase is recorded by all species, although notably least strongly by *C. wuellerstorfi* (~ 20.5 cal. kyr). Moreover, the good comparability of our epibenthic $\delta^{13}C$ record with other records from the North Atlantic (e.g., Sarnthein et al., 1994) certainly precludes bioturbational downmixing as a major cause too. It seems more likely that both factors, the specific ecological behaviour of each benthic species to changes in water mass/food supply as well as the relatively high time span of 550 yr covered by each of our glacial samples are responsible for the two very different benthic $\delta^{18}O$ records. This means that the two benthic species may not have lived at the same time and, therefore, may not represent exactly the same bottom conditions. Because the total number of tests of *C. wuellerstorfi* found in the glacial samples is considerably less compared with *O. umbonatus*, the rare occurrence of *C. wuellerstorfi* may represent relatively short-lived events whereas *O. umbonatus* better reflects long-term changes. Considering that *C. wuellerstorfi* is a suspension feeder relying on interglacial-like conditions it probably responded quickly by growing its test at times when water-mass conditions and food supply resembled more closely an interglacial mode. That overall environmental conditions during the LGM were very special also at the seafloor is certainly corroborated by the time-restricted and unusual occurrence of *S. rolshauseni*. Although the sudden appearance of this species is difficult to explain as it has no modern analogue to compare with, its stratigraphic range seems clearly correlated to major events recognized in most of our other environmental proxy records (see Fig. 5).

6.2. Early deglaciation

After the LGM, the first major minimum in the planktic $\delta^{18}O$ record (~ 18 cal. kyr) has been related to the early melting of the Barents Sea ice sheet (Jones and Keigwin, 1988). The timing seems consistent with dates reported for the retreat of this ice sheet from the shelf break (Elverhøi et al., 1995; Svendsen et al., 1996; Vorren and Laberg, 1996). Although this $\delta^{18}O$ spike is roughly coeval in time with the H1 cold event in the North Atlantic, in our and other records from the Nordic seas (Elverhøi et al., 1995; Dokken and Hald, 1996) this event is not associated with enhanced fluxes of IRD (see also Stein et al., 1996). Various hypotheses, such as isostatic depression or sudden sea-level rise in combination with increased postglacial warming have been proposed by several authors to explain this early $\delta^{18}O$ depletion (Jones and Keigwin, 1988; Forman et al., 1995; Polyak et al., 1995). The timing of this event (or time correlatives of it) also reveals some kind of regional patchiness. Apart from the central Arctic Ocean, around Spitsbergen and along East Greenland (Jones and Keigwin, 1988; Stein et al., 1994), it is also recognizable in the northern Denmark Strait (Voelker et al., 1998) where faunal and isotopic downcore data reveal that warm Atlantic water existed here during early deglaciation (Sarnthein et al., 1995; Voelker et al., 1998). Therefore, it could well be that during early Termination I surface warming first occurred along eastern Greenland and the central Nordic seas (cf. Sarnthein et al., 1995). This would explain the consistently younger ages of the first major postglacial $\delta^{18}O$ depletion found in cores from off western Norway (e.g., Weinelt et al., 1991). In any case, this early $\delta^{18}O$ event in core PS1243 seems to have merged with episodes of increased meltwater discharge occurring in the Norwegian Sea about 1 kyr later (Sarnthein et al., 1995). The low benthic and planktic $\delta^{13}C$ values reveal that vertical convection was extremely reduced during this time, conditions which remained like this until about 15 cal. kyr. Thereafter, IRD fluxes indicate a notable increase in iceberg activity centred around 14 cal. kyr (Fig. 6). This IRD increase is time-coeval with glacier advances in northwestern Norway and Spitsbergen (Vorren and Elvsborg, 1979; Mangerud et al., 1992). Because this event at 14 cal. kyr is associated with enhanced flux rates in both crystalline and clastic IRD, we assume that Spitsbergen and/or parts of the relatively shallow northwestern Barents Sea were the most likely region that became affected by this renewed ice advance (Svendsen et al., 1996).

The final phase of the early deglaciation prior to the YD is marked by an initial but remarkable major surface warming centred at about 13.5 cal. kyr, which seems to represent the Bølling/Allerød period (Fig. 6). The relatively high number of subpolar foraminifera reflect Holocene-like water-mass conditions in the Nordic seas. This time is associated with high benthic $\delta^{13}C$ and $\delta^{18}O$ values (highest $\delta^{18}O$ values are now observed in *C. wuellerstorfi* since the beginning of full-glacial conditions at 26 cal. kyr). In strict accordance with previous interpretations based on cores from outside the Nordic seas (Lehman and Keigwin, 1992; Sarnthein et al., 1994), the significant increase in epibenthic $\delta^{18}O$ and $\delta^{13}C$ which gradually began already after 15 cal. kyr should, therefore, be regarded as evidence for the change from the typical glacial circulation (i.e., subsurface inflow of upper Atlantic water) to the modern open-ocean circulation style with increasingly more oceanic heat being pumped into the still rather cold subarctic latitudes. This oceanic change eventually caused a deeper reaching vertical convection in the central Nordic seas, leading to enhanced NADW production for the North Atlantic and decreased bottom temperatures in the Nordic seas. Although the abundance record of *C. wuellerstorfi* first increased $\sim$ 18 cal. kyr (Fig. 4), a notable surface warming in the region of site PS1243 has not occurred before 15 cal. kyr. In the southeastern Norwegian Sea, for comparison, plankton data reveal first surface warming at $\sim$ 16 cal. kyr (Lehman and Keigwin, 1992; Koç-Karpuz and Jansen, 1992), matching in timing quite well the major change in our *C. wuellerstorfi* record as well as in the Greenland ice core (Figs. 4 and 6).

6.3. Younger Dryas

From the point of paleoceanography, there are several hitherto unanswered questions regarding the YD cold event which occurred during times of maximum insolation (Fig. 6). One of these is related to whether this cooling was possibly triggered by lowered surface ocean salinities during the course of ice-sheet melting (Broecker et al., 1990). Another one concerns the consequences of this event for the contemporaneous ocean circulation in the North Atlantic. This second question has been controversial. Based on epibenthic foraminiferal $\delta^{13}C$, some authors have found evidence for a significant decrease (i.e., lowered $\delta^{13}C$) in NADW production (e.g., Boyle and Keigwin, 1987; Keigwin and Lehman, 1994) whereas others could not support such a finding (e.g., Jansen and Veum, 1990; Sarnthein et al., 1994). Our epibenthic $\delta^{13}C$ record around the YD event is very similar to data from the southeastern Norwegian Basin published by Veum et al. (1992). But the record of core PS1243 seems more detailed, showing that around 13 cal. kyr, just before the onset of the YD but clearly after the Bølling/Allerød warming, there was a notable depletion in epibenthic $\delta^{13}C$ which seems coeval in time with a massive planktic $\delta^{18}O$ in the Fram Strait. The very high epibenthic $\delta^{13}C$ values observed later during the first part of the YD were associated with a high accumulation of IRD as well as cold surface water in the Nordic seas and cold air temperature over Greenland (Fig. 6). The high $\delta^{13}C$ values should be interpreted as the result of increased rates of vertical convection in the Nordic seas whereas the depletions by 0.5‰ observed at near the beginning and the end of the YD would imply a slowdown of this convectional process. Inferred lower rates of vertical convection during these two depletions could have been caused by meltwater at the surface. At face value, the strong decrease in planktic $\delta^{18}O$ identified in the western Fram Strait at the beginning of the YD would point to the Arctic Ocean freshwater system as triggering cause for the YD (Bauch et al., 2000b), because this $\delta^{18}O$ event is not recognized in the Nordic seas (Fig. 6; see also Sarnthein et al., 1995). The conclusion that the Arctic might have triggered the YD seems intriguing but remains speculative at present as additional cores would be required from this high-northern region for confirmation, however, with a higher temporal resolution than PS1230.

So, do the epibenthic $\delta^{13}C$ values of 1.6–1.1‰ during the YD really reflect fast surface water overturning? As was demonstrated, the 2 cm thick layer of the Vedde Ash in core PS1243 documents instantaneous deposition during the volcanic eruption (Fig. 3). The radiocabon-dated base of this ash gave an uncorrected age of $10{,}630 \pm 150$ yr. Recently, dated plant material within the Vedde Ash horizon in southern Norway has revealed an age of 10,300 yr (Bard et al., 1994; Birks et al., 1996), directly reflecting the atmospheric ^{14}C of this time. After correcting our date below the Vedde Ash for the well-known ^{14}C plateau and a reservoir effect of 400 yr, the calendar age for the Vedde Ash of $\sim$ 12 cal. kyr in core PS1243 (Fig. 6) is comparable to the age of the tephra calculated on the basis of counted annual layers in the GRIP ice core (Grønvold et al., 1995). Hence, our age for the Vedde Ash corroborates both a relatively small reservoir age of $\sim$ 300–400 yr and, as also supported by the increased epibenthic $\delta^{13}C$ just below the ash, a relatively high rate in vertical convection in the central Nordic seas during this time. Our ^{14}C reservoir estimate for the central Nordic seas is significantly less than the 700–800 yr recently calculated by Bard et al. (1994) for the North Atlantic using a similar approach, however, on the basis of ice-rafted ash particles. It is hard to reconcile the high epibenthic $\delta^{13}C$ values and small reservoir effect for the mid-YD relative to the late Holocene with a slowdown of the ocean conveyor, particularly, because this time was accompanied by low $\delta^{18}O$ values in *N. pachyderma* sin. and *O. umbonatus* (Fig. 6). It therefore may well be that the changes in deep-sea epibenthic $\delta^{13}C$ records are at times also affected by other factors than just intensity in water-mass ventilation, e.g., such as the rate in vertical food flux and air-sea exchange (Charles et al., 1993; Mackensen et al., 1993).

6.4. Late deglaciation

The interval directly after the YD is still characterized by relatively low epibenthic $\delta^{13}C$ values indicating that the intensity of vertical convection was still reduced. Although the relative abundance in polar foraminifera generally decreased during this phase (Figs. 5 and 6), in more detail the planktic data reveal a notable warming and subsequent surface cooling centred at ~11 and 10.5 cal. kyr, respectively. Similar events have been recently reported also from the northeastern Norwegian Sea (Hald and Hagen, 1998).

The common picture of still unstable trends persisted in all of our proxy records until ~10 cal. kyr when IRD deposition ceased in the central Nordic seas and, with a time lag of ~1 kyr, also in the Fram Strait area. The fact that the two benthic $\delta^{18}O$ records show consistently the same values only after the IRD had vanished may be taken as evidence for the establishment of normal marine salinities at the surface and the onset of a consistent thermohaline circulation system. From this time onwards warm surface-water conditions rapidly evolved in most areas of the Nordic seas (Koç et al., 1993; Bauch et al., 1999), which was concomitant with atmospheric changes over Greenland and Scandinavia (Fig. 6; Nesje and Kvamme, 1991).

6.5. Holocene

The further development of the water-mass conditions in the Nordic seas after 10 cal. kyr is marked by a significant cooling centred at ~8 cal. kyr (Fig. 6). Although not very well constrained by our ^{14}C dates in core PS1243, this cooling seems related to the brief event recognized in the GRIP and GISP2 ice cores at 8.2 cal. kyr (Alley et al., 1997). In core PS1243 this event is associated with low epibenthic $\delta^{13}C$ values, implying decreased ventilation in the Nordic seas. Although freshwater from melting icebergs in the Nordic seas must be ruled out because of the lack of IRD, this cooling was probably still induced by significant surface ocean changes which were triggered by the final episode of the Fennoscandian and Laurentide deglaciation (Bauch and Weinelt, 1997; Barber et al., 1999).

Warmest surface conditions were reached in the central Nordic seas around 7 cal. kyr when the dominance of subpolar foraminiferal species was strongest (Fig. 6). This was also the time when the water-mass/sea-ice conditions in the Fram Strait became comparable to the modern situation, i.e., the in- and outflow of Atlantic (WSC) and polar waters (EGC), respectively. Higher planktic $\delta^{13}C$ values are commonly observed in surface sediments along the east Greenland margin than elsewhere in the Nordic seas (Weinelt, 1993; Johannessen et al., 1994; Hebbeln et al., 1998), and by far the highest values are found in the central Arctic Ocean (Spielhagen and Erlenkeuser, 1994). In addition, it has been observed in areas with long seasonal ice coverage but high summer bioproductivity that corrosive bottom waters may be formed via remineralization of organic matter (Steinsund and Hald, 1994). Thus, the assumption may be drawn that the high planktic $\delta^{13}C$ values in conjunction with increased carbonate corrosion recorded in core PS1230 for the past 7 cal. kyr reflect relatively stable and modern-like environmental conditions at the Arctic gateway.

Since about 6 cal. kyr, our records from core PS1243 and other surface ocean data from this region (e.g., Koç et al., 1993) suggest rather continuous surface cooling whereas the epibenthic $\delta^{13}C$ values, which finally approached the modern level of 1.3–1.4‰ shortly after, indicate unchanged strong vertical convection during the past 5 cal. kyr. The fact that surface cooling began while vertical convection remained on very high level implicates that the warmest surface conditions in the Nordic seas, which occurred between 10 and 6 cal. kyr, were probably also not directly related to intensified deep-water formation. More likely, the warm conditions in the early Holocene were the result of high insolation, ice-free conditions, and no significant meltwater input. On this basis, it may be further concluded that the present oceanographic situation, with the establishment of the Arctic and Polar frontal zones (Fig. 1), is the result of this last oceanic development. This finding is in contrast to other paleoceanographic conclusions in which the post-glacial water-mass evolution in the northern Atlantic region is believed as mere shifts in the geographical position of apparently rather time-persistent oceanographic fronts (e.g., Ruddiman and McIntyre, 1981; Fronval et al., 1998).

7. Conclusions

Using a multiproxy approach on a sediment core from the central Nordic seas (supported by data from a core at the Arctic gateway), the paleoenvironmental evolution of the deep and surface-water circulation was reconstructed for the last 30 cal. kyr. The records reveal that different styles of thermohaline circulation have occurred during glacial, deglacial, and interglacial periods, controlling the intensities of both northerly ocean heat flux and formation of NADW as well as the variability of ice-sheet growth on the landmasses surrounding the Nordic seas.

- Towards the end of OIS 3 (until 26 cal. kyr), open-water convection in the Nordic seas, as verified through high epibenthic $\delta^{13}C$ values, provided sufficient moisture supply from the North Atlantic for the Fennoscandian-Barents ice sheets to grow until they approached the shelf break at ~26 cal. kyr and started to deliver high amounts of IRD into the ocean via melting icebergs. All three $\delta^{18}O$ records show a parallel increase during this time, implying that the environment in the Nordic seas became increasingly glacial and that ice-sheet growth occurred on a global and regional scale until ~19 cal. kyr.
- On the basis of high fluxes of IRD between 26 and 19 cal. kyr, and the assumption that surface-water stratification prevailed due to low-density meltwater lids in

summer and sea-ice cover during the rest of the year, it is suggested that the advection of Atlantic water (down to intermediate water depths) into the Nordic seas occurred mainly at the subsurface, partly faciliated through polynyas. These polynyas, which were generated along the Fennoscandian-Barents ice sheets by catabatic winds, not only provided moisture to the ice sheets through upwelling of relatively warm Atlantic water, they may also have been responsible for the occurrence of small-sized subpolar foraminifera as far north as the Arctic Ocean. It is further suggested that this advection of relatively warm and saline Atlantic water at the subsurface in combination with supercooled $\delta^{18}O$ depleted surface water was also instrumental for the unusually light epibenthic $\delta^{18}O$ values observed during OIS 2.

- Despite a parallel decrease in planktic and benthic $\delta^{18}O$ records between 20 and 18 cal. kyr, which was probably mainly caused by a rapidly collapsing Barents Sea ice sheet due to sea-level rise in association with increasing atmospheric temperatures and solar radiation, glacial conditions characterized by a dominant thermohaline subsurface circulation prevailed until 15 cal. kyr. Thereafter, conditions rapidly improved, and after an intermittent brief cooling at about 14 cal. kyr, Holocene-like conditions with normal marine salinities and vertical overturning of inflowing Atlantic surface-water masses were established for the first time in the Bølling/Allerød (at 13.5 cal. kyr).
- The Younger Dryas cooling (YD) which followed the Bølling/Allerød warming was associated with enhanced IRD accumulation in the Nordic seas. Although very high epibenthic $\delta^{13}C$ values combined with a ^{14}C reservoir effect of just 300–400 yr, verify strong vertical water-mass convection during the first-half of the YD, this major cold phase was clearly preceded by notable depletion in both epibenthic $\delta^{13}C$ in the central Nordic seas and planktic $\delta^{18}O$ in the Fram Strait, implying a reduction in thermohaline circulation possibly caused by meltwater input from the Arctic Ocean.
- Another reduction in the rate of vertical water-mass convection is observed towards the end of the YD and into Preboreal times (12–10.5 cal. kyr). During this entire interval thermohaline circulation remained unstable, probably due to variations in meltwater input from the rapidly decaying ice sheets at the end of the deglaciation.
- Freshwater input into the central Nordic seas derived from melting icebergs completely ceased at 10 cal. kyr. Supported by strong atmospheric warming these improved surface-water conditions led to a strong surface-water warming which more or less persisted until about 6 cal. kyr.
- The warmest interval between 10 and 6 cal. kyr is interrupted by a slight depletion in epibenthic $\delta^{13}C$ values concordant with increased polar foraminiferal abundance centred around 8 cal. kyr. This event gives evidence of another notable surface water cooling in the central Nordic seas. Although the actual cause for this water mass change is not fully understood, it is most likely related to an entrainment of relatively fresh water into the thermohaline system caused by the final episode of northern hemisphere ice melting.
- After 7 cal. kyr the modern-type circulation started to evolve in the Nordic seas. This situation is characterized by the strong inflow of Atlantic water masses along the eastern Nordic seas into the Arctic Ocean, and the northerly outflow of cold polar waters along the Greenland continental margin. Although the intensity of deep-water formation has not changed during the last 5 ka, surface water temperatures began to decrease progressively already after 7 cal. kyr. This development eventually led to the modern steep east-to-west temperature gradients and the establishment of today's main water-mass boundaries.

Acknowledgements

We are grateful to the shipboard crews and scientists of RV *Polarstern* for collecting the two studied sediment cores from the Nordic seas. We also like to thank Anders Elverhøi and one anonymous reviewer for their valuable comments and A. Voelker and M. Weinelt for discussions. Thanks are expressed to the people from the Leibniz Laboratory (Kiel) who assisted in the numerous isotope measurements. This study was funded by the German Ministry for Science and Technology (*Paläoklimaprojekt)* and the Deutsche Forschungsgemeinschaft (*SFB 313*).

References

Alley, R., Mayewski, P.A., Sowers, T., Stuiver, M., Taylor, K.C., Clark, P.U., 1997. Holocene climatic instability: a prominent, widespread event 8200 yr ago. Geology 25, 483–486.

Barber, D.C., Dyke, A., Hillaire-Marcel, C., Jennings, A.E., Andrews, J.T., Kerwin, M.W., Bilodeau, G., McNeely, R., Southon, J., Morehead, M.D., Gagnon, J.-M., 1999. Forcing of the cold event of 8,200 years ago by catastrophic drainage of Laurentide lakes. Nature 400, 344–348.

Bard, E., Arnold, M., Mangerud, J., Paterne, M., Labeyrie, L., Duprat, J., Meliere, M.-A., Soenstegaard, E., Duplessy, J.-C., 1994. The North Atlantic atmosphere-sea surface ^{14}C gradient during the Younger Dryas climatic event. Earth and Planetary Science Letters 126, 275–287.

Bauch, H.A., 1992. Test size variation of planktic foraminifers as response to climatic changes. International Conference on Paleoceanography (ICP 4). GEOMAR Report 15, 56.

Bauch, H.A., 1994. Significance of variability in *Turborotalita quinqueloba* (Natland) test size and abundance for paleoceanographic interpretations in the Norwegian-Greenland Sea. Marine Geology 121, 129–141.

Bauch, H.A., 1997. Paleoceanography of the N. Atlantic Ocean (68°–78°N) during the past 450 ky deduced from planktic foraminiferal assemblages and stable isotopes. In: Hass, H.C., Kaminski, M.A. (Eds.), Contributions to the Micropaleontology and Paleoceanography of the Northern North Atlantic, Grzybrowski Foundation Special Publication, Vol. 5, Krakow, pp. 83–100.

Bauch, H.A., 1999. Planktic Foraminifera in Holocene sediments from the Laptev Sea and the Central Arctic Ocean: species distribution and paleobiogeographical implication. In: Kassens, H., et al. (Eds.), Land–Ocean Systems in the Siberian Arctic: Dynamics and History. Springer, New York, pp. 601–614.

Bauch, H.A., Erlenkeuser, H., Grootes, P.M., Jouzel, J., 1996. Implications of stratigraphic and paleoclimatic records of the last interglaciation from the Nordic seas. Quaternary Research 46 (3), 260–269.

Bauch, H.A., Weinelt, M.S., 1997. Surface Water Changes in the Norwegian Sea During Last Deglacial and Holocene Times. Quaternary Science Reviews 16 (10), 1115–1124.

Bauch, H.A., Erlenkeuser, H., Fahl, K., Spielhagen, R.F., Weinelt, M.S., Andruleit, H., Henrich, R., 1999. Evidence for a steeper Eemian than Holocene sea surface temperature gradient between Arctic and sub-Arctic regions. Palaeogeography, Palaeoclimatology, Palaeoecology 145 (1–3), 95–117.

Bauch, H.A., Erlenkeuser, H., Helmke, J.P., Struck, U., 2000a. A paleoclimatic evaluation of marine oxygen isotope stage 11 in the high-northern Atlantic (Nordic seas). Global and Planetary Change 24, 27–39.

Bauch, H.A., Cremer, H., Kunz-Pirrung, M., 2000b. Siberian shelf sediments contain clues to paleoclimate forcing. EOS Transactions 81, 233/238.

Baumann, K.H., Matthiessen, J., 1992. Variations in surface water mass conditions in the Norwegian Sea: evidence from Holocene coccolith and dinoflagellate cyst assemblages. Marine Micropaleontology 20, 129–146.

Baumann, K.H., Lackschewitz, K.S., Mangerud, J., Spielhagen, R.F., Wolf-Welling, T.C.W., Henrich, R., Kassens, H., 1995. Reflections of Scandinavian ice sheet fluctuations in Norwegian sea sediments during the past 150,000 years. Quaternary Research 43, 185–197.

Belanger, P.E., 1982. Paleo-oceanography of the Norwegian-Sea during the past 130,000 years: Coccolithophorid and foraminiferal data. Boreas 11, 29–36.

Birgisdottir, L., 1991. Die paläo-ozeanographische Entwicklung der Island See in den letzten 550,000 Jahren. Report SFB 313. Kiel University 34, 1–112.

Birks, H.H., Gulliksen, S., Haflidason, H., Mangerud, J., Possnert, G., 1996. New radiocarbon dates for the Vedde Ash and the Saksunarvatn Ash from western Norway. Quaternary Research 45, 119–127.

Bischof, J., 1994. The decay of the Barents Sea ice-sheet as documented by Nordic Seas ice-rafted debris. Marine Geology 117, 35–55.

Bischof, J., Lund, J.J., Ecke, H.-H., 1997. Palynomorphs of ice-rafted clastic sedimentary rocks in Late Quaternary glacial marine sediments of the Norwegian Sea as provenance indicators. Palaeogeography, Palaeoclimatology, Palaeoecology 129, 329–360.

Bond, G., Lotti, R., 1995. Iceberg discharge into the North Atlantic on millenial time scales during the last glaciation. Science 276, 1005–1010.

Bond, G.C., Broecker, W., Johnsen, S., McManus, J., 1993. Correlations between climate records from North Atlantic sediments and Greenland ice Nature 365, 143–147.

Bondevik, S., Svendsen, J.I., Johnsen, G., Mangerud, J., Kaland, P.E., 1997. The Storegga tsunami along the Norwegian coast, its age and runup. Boreas 26, 29–53.

Boyle, E.A., Keigwin, L.D., 1987. North Atlantic thermohaline circulation during the past 200,000 years linked to high-latitude surface temperature. Nature 330, 35–40.

Broecker, W.S., Andree, M., Bonani, G., Wolfli, W., Oeschger, H., Klas, M., 1988. Can the Greenland climatic jumps be identified in records from ocean and land? Quaternary Research 30, 1-6.

Broecker, W.S., Bond, G., Klas, M., 1990. A salt oscillator in the glacial Atlantic? Paleoceanography 5, 469–477.

Budéus, G., Schneider, W., Krause, G., 1998. Winter convection events and bottom water warming in the Greenland Sea. Journal of Geophysical Research 103 (C9), 18,513-18,527.

Carstens, J., Hebbeln, D., Wefer, G., 1997. Distribution of planktic foraminifera at the ice margin in the Arctic (Fram Strait). Marine Micropaleontology 29, 257–269.

Charles, C.D., Wright, J.D., Fairbanks, R.G., 1993. Thermodynamic influences on the marine carbon isotope record. Paleoceanography 8 (6), 691–697.

Corliss, B.H., 1985. Microhabitats of benthic foraminifera within deep-sea sediments. Nature 314, 435–438.

Costello, O., Bauch, H.A., 1997. Late Pleistocene–Holocene productivity record of benthic foraminifera from the Iceland Plateau. In: Hass, H.C., Kaminski, M.A. (Eds.), Contributions to the Micropaleontology and Paleoceanography of the Northern North Atlantic, Grzybrowski Foundation Special Publication, Vol. 5, Krakow, pp. 141–148.

Dokken, T.M., Hald, M., 1996. Rapid climatic shifts during isotope stages 2-4 in the polar north Atlantic. Geology 24 (7), 599–602.

Dokken, T.D., Jansen, E., 1999. Rapid changes in the mechanism of ocean convection during the last glacial period. Nature 401, 458–461.

Dowdeswell, J.A., Elverhoi, A., Andrews, J.T., Hebbeln, D., 1999. Asynchronous deposition of ice-rafted layers in the Nordic seas and North Atlantic Ocean. Nature 400, 348–351.

Duplessy, J.C., Labeyrie, L., Juillet, A., Maitre, F., Duprat, J., Sarnthein, M., 1991. Surface salinity reconstruction of the North Atlantic Ocean during the last glacial maximum Oceanologica Acta 14, 311–324.

Duplessy, J.C., Labeyrie, L., Blanc, P.L., 1988. Norwegian Sea Deep Water variations over the last climatic cycle: Paleo-oceanographical implications. In: Wanner, H., Siegenthaler, U. (Eds.), Long and Short Term Variability of Climate. Springer, New York, pp. 83–116.

Elverhøi, A., Andersen, E.S., Dokken, T., Hebbeln, D., Spielhagen, R.F., Svendsen, J.I., Sørflaten, M., Rørnes, A., Hald, M., Forsberg, C., 1995. The growth and decay of the late Weichselian ice sheet in western Svalbard and adjacent areas based on provenance studies of marine sediments. Quaternary Research 44, 303–316.

Environmental Working Group, 1998. Oceanography atlas for the summer period. In: Timokhov, L., Tanis, F. (Eds.), Joint U.S. Russian Atlas of the Arctic Ocean, Version 1.0. University of Colorado, Boulder.

Fairbanks, R.G., 1989. A 17,000-year glacio-eustatic sea level record: influence of glacial melting rates on the Younger Dryas event and deep ocean circulation. Nature 342, 637–642.

Foldvik, A., Gammelsrød, T., 1988. Notes on Southern Ocean hydrography, sea-ice and bottom water formation. Palaeogeography, Palaeoclimatology, Palaeoecology 67, 3–17.

Forman, S., Lubinski, D., Miller, G., Snyder, J., Matishov, G., Korsun, S., Myslivets, V., 1995. Postglacial emergence and distribution of late Weichselian ice-sheet loads in the northern Barents and Kara seas. Russia, Geology 23 (2), 113–116.

Fronval, T., Jansen, E., Bloemendal, J., Johnsen, S., 1995. Oceanic evidence for coherent fluctuations in Fennoscandian and Laurentide ice sheets on millenium timescales. Nature 374, 443–446.

Fronval, T., Jansen, E., Haflidason, H., Sejrup, H.-P., 1998. Variability in surface and deep water conditions in the Nordic seas during the last interglacial period. Quaternary Science Reviews 17, 963–985.

Grønvold, K., Oskarsson, N., Johnsen, S.J., Clausen, H., Hammer, C.U., Bond, G., Bard, E., 1995. Ash layers from Iceland in the the Greenland GRIP ice core correlated with oceanic and land sediments. Earth and Planetary Science Letters 135, 149–155.

Hald, M., Dokken, T., Hagen, S., 1996. Palaeoceanography on the European arctic margin during the last deglaciation. In: Andrews, J.T., et al. (Eds.), Late Quaternary Palaeoceanography of the North Atlantic Margins, Vol. 111. Geological Society Special Publication, pp. 275–287.

Hald, M., Hagen, S., 1998. Early Preboreal cooling in the Nordic seas region triggered by meltwater. Geology 26, 615–618.

Hebbeln, D., Dokken, T., Andersen, E.S., Hald, M., Elverhoi, A., 1994. Moisture supply for northern ice-sheet growth during the Last Glacial Maximum. Nature 370, 357–360.

Hebbeln, D., Henrich, R., Baumann, K.-H., 1998. Paleoceanography of the last interglacial/glacial cycle in the Polar North Atlantic. Quaternary Science Reviews 17, 125–153.

Gard, G., 1993. Late Quaternary coccoliths at the North Pole: evidence of ice-fre conditions and rapid sedimentation in the central Arctic Ocean. Geology 21, 227–230.

Imbrie, J., Berger, A., Boyle, E.A., Clemens, S.C., Duffy, A., Howard, W.R., Kukla, G., Kutzbach, J., Martinson, D.G., McIntyre, A., Mix, A.C., Molfino, B., Morley, J.J., Peterson, L.C., Pisias, N.G., Prell, W.L., Raymo, M.E., Shackleton, N.J., Toggweiler, J.R., 1993. On the structure and origin of major glaciation cycles: 2. The 100,000-year cycle. Paleoceanography 8 (6), 699–735.

Jansen, E., Bjørklund, K.R., 1985. Surface ocean circulation in the Norwegian Sea, 15,000 B.P. to present. Boreas 14, 243–257.

Johannessen, T., Jansen, E., Flatøy, A., Ravelo, A., 1994. The relationship between surface water masses, oceanographic fronts and paleoclimatic proxies in surface sediments of the Greenland, Iceland, Norwegian Seas. In: Zahn, R., Pedersen, T.F., Kaminski, M.A., Labeyrie, L. (Eds.), Carbon Cycling in the Glacial Ocean: Constraints of the Ocean's Role in Global Change. Springer, Berlin, pp. 61–85.

Jones, G.A., Keigwin, L.D., 1988. Evidence from Fram Strait (78°) for early deglaciation. Nature 336, 56–59.

Keigwin, L.D., Lehman, S.J., 1994. Deep circulation change linked to HEINRICH event 1 and Younger Dryas in a middepth North Atlantic core. Paleoceanography 9 (2), 185–194.

Kellogg, T.B., 1980. Paleoclimatology and paleoceanography of the Norwegian and Greenland Seas: glacial-interglacial contrasts. Boreas 9, 115–137.

Kellogg, T.B., 1984. Paleoclimatic significance of subpolar foraminifera in high-latitude marine sediments. Canadian Journal of Earth Science 21, 189–193.

Knies, J., Stein, R., 1998. New aspects of organic carbon deposition and its paleoceanographic implications along the northern Barents Sea margin during the last 30,000 years. Paleoceanography 13, 384–394.

Koç-Karpuz, N., Jansen, E., 1992. A high-resolution diatom record of the last deglaciation from the SE Norwegian Sea; documentation of rapid climatic changes. Paleoceanography 7 (4), 499–520.

Koç, N., Jansen, E., Haflidason, H., 1993. Paleoceanograhic reconstructions of surface ocean conditions in the Greenland, Iceland and Norwegian Seas through the last 14 ka based on diatoms. Quaternary Science Reviews 12, 115–140.

Koç, N., Jansen, E., 1994. Response of the high-latitude Northern Hemisphere to orbital climate forcing: evidence from the Nordic Seas. Geology 22, 523–526.

Laberg, J., Vorren, T., 1995. Late Weichselian submarine debris flow deposits on the Bear Island Trough mouth fan. Marine Geology 127, 45–72.

Lehman, S.L., Keigwin, L.D., 1992. Sudden changes in North Atlantic circulation during the last deglaciaton. Nature 356, 757–762.

Mackensen, A., Hubberten, H.-W., Bickert, T., Fischer, G., Fütterer, D.K., 1993. The $\delta^{13}C$ in benthic foraminiferal tests of *Fontbotia wuellerstorfi* (Schwager) relative to the $\delta^{13}C$ of dissolved inorganic carbon in southern ocean deep water: implications for glacial ocean circulation models. Paleoceanography 8 (5), 587–610.

Mangerud, J., Bolstad, M., Elgersma, A., Helliksen, D., Landvik, J.Y., Lønne, I., Lycke, A.K., Salvigsen, O., Sandahl, T., Svendsen, J.I., 1992. The last glacial maximum on Spitsbergen, Svalbard. Quaternary Research 38, 1–31.

Maslin, M.A., Shackleton, N.J., Pflaumann, U., 1995. Surface water temperature, salinity, and density changes in the northeast Atlantic during the past 45,000 years: Heinrich events, deep water formation, and climatic rebounds. Paleoceanography 10 (3), 527–544.

Matthiessen, J., 1995. Distribution patterns of dinoflagellate cysts and other organic-walled microfossils in recent Norwegian-Greenland Sea sediments. Marine Micropaleontology 24, 307–334.

McCorkle, D.C., Keigwin, L.D., 1994. Depth profiles of $\delta^{13}C$ in bottom water and core top C. wuellerstorfi on the Ontong Java Plateau and Emperor Seamount. Paleoceanography 9 (2), 197–208.

Meese, D., Alley, R., Gow, T., Grootes, P.M., Mayewski, P., Ram, M., Taylor, K., Waddington, E., Zielinski, G., 1994. Preliminary depth-age scale of the GISP2 ice core. CRREL Special Report, 94–101.

Nees, S., Struck, U., 1994. The biostratigraphic and paleoceanographic significance of Siphotextularia roslhauseni Phleger and Parker in Norwegian-Greenland Sea sediments. Journal of Foraminiferal Research 24 (4), 233–240.

Nesje, A., Kvamme, M., 1991. Holocene glacier and climate variations in western Norway: evidence for early Holocene glacier demise and multiple Neoglacial events. Geology 19, 610–612.

Nähr-Hagen, H., 1993. Dinoflagellate cyst stratigraphy of the Barremian to Albian, lower Cretaceous. North-East Greenland Geologiske Undersögelse Bulletin 166, 1–171.

Nørgaard-Pedersen, N., Spielhagen, R.F., Thiede, J., Kassens, H., 1998. Central Arctic surface ocean environment during the past 80,000 years. Paleoceanography 13 (2), 193–204.

Okulitch, A.V., Lopatin, B.G., Jackson, H.R., 1989. Circumpolar map of the Arctic, Geological Survey of Canada, Map 1765 A.

Polyak, L., Lehman, S.J., Gataullin, V., Jull, T.A.J., 1995. Two-step deglaciation of the southeastern Barents Sea. Geology 23 (6), 567–571.

Rahmstorf, S., 1995. Bifurcations of the Atlantic thermohaline circulation in response to changes in the hydrological cycle. Nature 378, 145–149.

Rasmussen, T.L., Thomsen, E., van Weering, T.C.E., Labeyrie, L., 1996. Rapid changes in surface and deep waters at the Faeroe Margin during the last 58,000 years. Paleoceanography 11, 757–771.

Ruddiman, W.F., McIntyre, A., 1981. The North Atlantic Ocean during the last deglaciation. Paleogeography, Paleoclimatology, Paleoecology 35, 145–214.

Sarnthein, M., Winn, K., Jung, S.J.A., Duplessy, J.-C., Labeyrie, L., Erlenkeuser, H., Ganssen, G., 1994. Changes in east Atlantic deepwater circulation over the last 30,000 years: eight time slice reconstructions. Paleoceanography 9 (2), 209–267.

Sarnthein, M., Jansen, E., Weinelt, M.S., Arnold, M., Duplessy, J.-C., Erlenkeuser, H., Flatøy, A., Johannessen, G., Johannessen, T., Jung, S., Koç, N., Labeyrie, L., Maslin, M., Pflaumann, U., Schulz, H., 1995. Variations in Atlantic surface ocean paleoceanography, 50°–80°N: A time-slice record of the last 30,000 years. Paleoceanography 10 (6), 1063–1094.

Spielhagen, R.F., 1991. Die Eisdrift in der Franstraße während der letzhen 200.000 Jahre, GEOMAR Rep. 4, 133.

Spielhagen, R.F., Erlenkeuser, H., 1994. Stable oxygen and carbon isotopes in planktic foraminifers from Arctic ocean surface sediments: Reflection of the low salinity surface water layer. Marine Geology 119, 227–250.

Stein, R., Nam, S.-I., Schubert, C., Vogt, C., Fütterer, D., Heinemeier, J., 1994. The last deglaciation event in the eastern Central Artic Ocean. Science 264, 692–696.

Stein, R., Nam, S.-I., Grobe, H., Hubberten, H., 1996. Late Quaternary glacial history and short-term ice-rafted debris fluctuations along the East Greenland continental margin. In: Andrews, J.T., Austin, W.E.N., Bergsten, H., Jennings, A.E. (Eds.), Late Quaternary palaeoceanography of the North Atlantic Margins, Vol. 111. Geological Society Special Publication, pp. 135–151.

Steinsund, P.I., Hald, M., 1994. Recent calcium carbonate dissolution in the Barents Sea: paleoceanographic implications. Marine Geology 117, 303–316.

Struck, U., 1995. Stepwise post-glacial migration of benthic foraminifera into the abyssal NE Norwegian Sea. Marine Micropaleontology 26, 207–213.

Stuiver, M., Reimer, P.J., 1993. Extended ^{14}C database and revised CALIB radiocarbon calibration program. Radiocarbon 35, 215–230.

Taylor, K.C., Hammer, C.U., Alley, R.B., Clausen, H.B., Dahl-Jensen, D., Gow, A.J., Gundestrup, N.S., Kipfstuhl, J., Moore, J.C., Waddington, E.D., 1993. Electrical conductivity measurements from the GISP2 and GRIP Greenland ice cores. Nature 366, 549–554.

Veum, T., Jansen, E., Arnold, M., Beyer, I., Duplessy, J.-C., 1992. Water mass exchange between the North Atlantic and the Norwegian Sea during the past 28,000 years. Nature 356, 783–785.

Vidal, L., Labeyrie, L., van Weering, T.C.E., 1998. Benthic $\delta^{18}O$ records in the North Atlantic over the last glacial period (60–10kyr): evidence for brine formation. Paleoceanography 13 (3), 245–251.

Voelker, A.H.L., Sarnthein, M., Grootes, P.M., Erlenkeuser, H., Laj, C., Nadeau, M.-J., Schleicher, M., 1998. Correlation of marine ^{14}C ages from the Nordic seas with the GISP2 isotope record: implications for radiocarbon calibration beyond 25 ka BP. Radiocarbon 1, 517–534.

Vorren, T.O., Elvsborg, A., 1979. Late Weichselian deglaciation and paleoenvironment of the shelf and coastal areas off Tromso, north Norway — a review. Boreas 8, 247–253.

Vorren, T.O., Laberg, J.S., 1996. Late glacial air temperature, oceanographic and ice sheet interactions in the southern Barents Sea region. In: Andrews, J.T., Austin, W.E.N., Bergsten, H., Jennings, A.E., Late Quaternary Palaeoceanography of the North Atlantic Margins. Geological Society Special Publication, Vol. 111, 303–321.

Wagner, T., Henrich, R., 1994. Organo- and lithofacies of glacial-interglacial deposits in the Norwegian–Greenland Sea: responses to paleoceanographic and paleoclimatic changes. Marine Geology 120, 335–364.

Weinelt, M.S., 1993. Veränderungen der Oberflächenzirkulation im Europäischen Nordmeer während der letzten 60,000 Jahre. Report SFB 313 Kiel University 41, 1–105.

Weinelt, M.S., Sarnthein, M., Vogelsang, E., Erlenkeuser, H., 1991. Early decay of the Barents Shelf Ice Sheet — spread of stable isotope signals across the eastern Norwegian Sea. Norsk Geologisk Tidsskrift 71, 137–140.

Weinelt, M., Sarnthein, M., Pflaumann, U., Schulz, H., Jung, S., Erlenkeuser, H., 1996. Ice-free Nordic seas during the last glacial maximum?. Potential sites of Deepwater formation. Palaeoclimates 1, 283–309.

Zahn, R., Schönfeld, J., Kudrass, H.-R., Park, M.-H., Erlenkeuser, H., Grootes, P., 1997. Thermohaline instability in the North Atlantic during meltwater events: stable istope and ice-rafted detritus records from core SO75-26KL. Portuguese margin. Paleoceanography 12 (5), 696–710.